



THE UNIVERSITY OF  
**WAIKATO**  
*Te Whare Wānanga o Waikato*

Research Commons

<http://researchcommons.waikato.ac.nz/>

## Research Commons at the University of Waikato

### Copyright Statement:

The digital copy of this thesis is protected by the Copyright Act 1994 (New Zealand).

The thesis may be consulted by you, provided you comply with the provisions of the Act and the following conditions of use:

- Any use you make of these documents or images must be for research or private study purposes only, and you may not make them available to any other person.
- Authors control the copyright of their thesis. You will recognise the author's right to be identified as the author of the thesis, and due acknowledgement will be made to the author where appropriate.
- You will obtain the author's permission before publishing any material from the thesis.

**Evolution of *Bacillus subtilis*:  
A Novel Phenotype and its Challenges**

A thesis  
submitted in partial fulfilment  
of the requirements for the degree  
of  
**Master of Science (Research)**  
at  
**The University of Waikato**  
by  
**Mitchell John Murray**



THE UNIVERSITY OF  
**WAIKATO**  
*Te Whare Wānanga o Waikato*

2018

# Abstract

---

The enzyme LeuB from the last common ancestor of the firmicutes has been statistically recreated using several different methods. This project deals with two versions, Rec/LG and Rec/EX. To better understand these resurrected enzymes, the proteins were crystallised. Despite extensive efforts to produce crystals of diffraction quality, none of the crystals developed during this project were large enough to be of any use in X-Ray crystallography. Strains of *Bacillus subtilis* were genetically modified to each have one of either Rec/LG or Rec/EX in place of the native *leuB* gene, and then were allowed to evolve alongside an unmodified strain for 500 generations. Attempts were made to extract DNA from the evolved strains at different points throughout the evolution experiment for whole genome sequencing, and to amplify the *leuB* gene via PCR for direct comparisons of changes that may have occurred to the *leuB* gene over the course of the evolution experiment. These attempts were ultimately unsuccessful. In lieu of this genetic data, phenotypic changes to the evolved strains were characterised. A new phenotype appeared extremely early on in the experiment (by generation 54), and in less than 300 generations had swept to fixation in 9 independent strains. In all cases, this phenotype included poor growth on LB agar plates, small colonies, and small cells. Similar changes have been observed before in laboratory experiments of *B. subtilis*, but none occurred so quickly or so uniformly across independent samples.

# Acknowledgements

---

I'd like to thank everyone in C.2.10 for always being so friendly, patient, and helpful. You all made every day in the lab a joy, and I can't count the number of times someone helped me find something, make something, get something to work, or stopped me from breaking something. I would especially like to thank Dr. Vickery Arcus for making sure my project was always going in a direction that worked for me, Dr. Emma Andrews for helping me understand what I was doing and why, Dr. Erica Prentice for being my unofficial third supervisor and doing a damn good job at it, and Dr. Judith Burrows and Dr. Emma Summers for the tireless work they do to make sure the lab actually runs. I'd also like to thank Dr. Ray Cursons for helping me with my DNA extractions and PCR. Despite the setbacks, roadblocks, and problems with my project, this has been a great year, entirely because of how fun it is to work in this lab with you all.

Finally, I'd like to thank my parents, who tried so hard but just never quite got it.

# Table of Contents

---

## Contents

Abstract .....	ii
Acknowledgements .....	iii
Table of Contents .....	iv
List of Figures .....	vii
List of Tables.....	ix
1 1	
Introduction .....	1
1.1 Ancestral Sequence Reconstruction.....	1
1.2 The Use of ASR With LeuB Enzymes .....	3
1.2.1 ANC1-4 .....	3
1.2.2 Fitness Experiments .....	5
1.2.3 Rec/LG and Rec/EX.....	6
1.3 LeuB Structure and Function.....	7
1.3.1 Leucine Biosynthesis.....	7
1.3.2 Active Site of LeuB.....	8
1.3.3 Temperature and LeuB.....	10
1.4 Bacterial Evolution Experiments .....	11
1.4.1 A Brief Overview .....	11
1.4.2 Evolution in <i>Bacillus subtilis</i> .....	12
1.5 The Evolution of Rec/LG and Rec/EX .....	13
2 14	
Structure of Rec/LG and Rec/EX.....	14
2.1 Introduction.....	14
2.2 Methods .....	14
2.2.1 Protein Expression.....	14
2.2.2 Protein Purification .....	15

2.2.3	Robotic Crystallisation Screens .....	16
2.2.4	Fine Screens .....	16
2.2.5	Structure Modelling and Analysis.....	16
2.3	Results and Discussion .....	17
2.3.1	Crystallisation of Rec/LG and Rec/EX .....	17
2.3.2	Structure Models for Rec/LG and Rec/EX. ....	17
3	22	
	Genetics of the Evolution Experiment .....	22
3.1	Introduction.....	22
3.2	Methods and Method Development.....	22
3.2.1	Genomic DNA Extraction.....	22
3.2.2	PCR Amplification of the <i>LeuB</i> Gene.....	24
3.2.3	DNA Quality .....	25
3.3	Results.....	26
3.3.1	Genomic DNA Extraction.....	26
3.3.2	PCR Amplification of the <i>LeuB</i> Gene.....	28
3.3.3	Heterogeneity of Evolved Samples .....	29
	Morphology of Evolved <i>Bacillus subtilis</i> .....	30
4.1	Introduction.....	30
4.2	Methods .....	30
4.2.1	Plate Growth.....	30
4.2.2	Endospore Staining .....	30
4.3	Results.....	31
4.3.1	Colony Morphology .....	31
4.3.2	Growth of the New Morphotype .....	33
4.3.3	Sporulation and Cell Morphology.....	34
	Discussion and Future Research .....	38
5.1	Structure of Rec/LG and Rec/EX .....	38

5.2 Genetics of Evolved Samples .....	39
5.2.1 Whole Genome DNA Extraction .....	39
5.2.2 PCR Amplification of <i>leuB</i> .....	40
5.3 Morphology of Evolved <i>Bacillus subtilis</i> .....	41
5.3.1 Phenotypic Differences Between Samples.....	41
5.3.2 Comparing NCM to SCV .....	42
5.4 Conclusions.....	44
References .....	45
Appendix .....	53

# List of Figures

---

Figure 1: Schematic of the branched-chain amino acid (BCAA) biosynthesis pathway in <i>Ralstonia eutropha</i> , including the biosynthesis of leucine from 2-ketoisovalerate (Brigham et al., 2015).....	8
Figure 2: Isopropylmalate (left) and Isocitrate (right). The different groups attached to the $\gamma$ carbon appear to be crucial in the substrate specificity of LeuB. Chemical structure images retrieved from <a href="https://pubchem.ncbi.nlm.nih.gov">https://pubchem.ncbi.nlm.nih.gov</a> on 17.10.2017.....	9
Figure 3: The substrate binding site of LeuB, complexed with IPM (green). Glu88 (pink) creates a negative charge at the mouth of the hydrophobic binding pocket which prevents binding of isocitrate. Leu91, Leu92, and Val193 (blue) all contribute to the formation of the hydrophobic binding pocket. Adapted from Imada et al. 1998.....	10
Figure 4: Pictures of protein crystals of Rec/LG and Rec/EX. See appendix for crystallisation conditions. ....	17
Figure 5: B factor putty cartoons of A: The Rec/LG model and B: The Rec/EX model, using SWISS-MODEL's local quality estimate in place of B factor values. Higher numbers, towards the red end of the colour spectrum, indicate a higher quality. ....	19
Figure 6: The near identical NAD binding sites of A: Rec/LG. B: Rec/EX. C: ANC4. The only residue not conserved between all three is circled in red. Position of NADH adapted from Graczer et al. 2011. Structure of ANC4 adapted from Hobbs et al. 2011. Note that the glutamic acid on the far right in A and B is also present in C, but it has not been properly represented in the crystal structure. ....	20
Figure 7: The active sites of Rec/LG (pink Carbons), Rec/EX (green Carbons), and ANC4 (blue Carbons) overlapping and shown as lines. Position of NADH (green Carbons) adapted from Graczer et al. 2011. Position of IPM (yellow Carbons) adapted from Imada et al. 1997. Structure of ANC4 adapted from Hobbs et al. 2011. ....	20
Figure 8: 1% agarose gel of genomic DNA extracted from the parents of W168, Rec/LG, and Rec/EX using the original method. ....	26
Figure 9: 1% agarose gel of genomic DNA extracted from Gen54 W168 samples, using the phenol chloroform based method. ....	27
Figure 10: 1% agarose gel of genomic DNA extracted from the parents of W168, Rec/LG, and Rec/Rec/EX using the optimised method. ....	28
Figure 11: Evolved samples from generation 54 grown on agar plates, illustrating differences in colony morphology. ....	31

Figure 12: Evolved samples from generation 199 grown on agar plates, illustrating differences in colony morphotype. ....	32
Figure 13: Evolved samples from generation 298 grown on agar plates, all displaying the NCM. ....	33
Figure 14: W168 samples from generation 298 after 24 hrs of growth on agar plates.....	33
Figure 15: W168 samples from generation 298 after 48 hrs of growth on agar plates.....	34
Figure 16: Cells from generation 54 after endospore staining. ....	35
Figure 17: Cells from generation 199 after endospore staining. ....	36
Figure 18: Cells from generation 298 after endospore staining. ....	37

# List of Tables

---

Table 1: One example of yield and purity of genomic DNA extracted from the parents of W168, Rec/Rec/LG, and Rec/EX using the original method.....	26
Table 2: Yield and purity of genomic DNA extracted from Gen54 W168 samples, using the phenol chloroform based method. ....	27
Table 3: Yield and purity of genomic DNA extracted from the parents of W168, Rec/LG, and Rec/EX using the optimised method.....	28

# 1

## Introduction

---

### 1.1 Ancestral Sequence Reconstruction

Ancestral Sequence Reconstruction (ASR) is a technique used to study the history, evolution, and function of proteins. The core concept of ASR involves gene sequencing for multiple related proteins, which are then aligned. From this sequence alignment, a phylogeny is generated. The nodes of this phylogeny represent various ancestral versions of the protein of interest spanning all the way back to the common ancestor of all the extant proteins involved in the analysis. The sequences of these nodes can be statistically inferred, generating an approximation of what the true ancestral proteins were like. The genes that code for these inferred sequences can then be synthesised, providing a physical reconstruction of ancient extinct proteins that can be subject to experimentation (Cai, Pei, & Grishin 2004; Merkl & Sterner 2016).

The uses of this technique are many and varied. First and most obviously, ASR can be used to study the history of proteins, offering a glimpse at the proteome of extinct organisms (Hobbs *et al.* 2011; Risso *et al.* 2013; Loughran *et al.* 2014). This can be extended into an inference of what the environment that these organisms lived in was like (Gaucher *et al.* 2003; Gaucher, Govindarajan, & Ganesh 2008). ASR can also be used as part of a “vertical approach” for studying protein structure and function. Ultimately, the information that can be gained from extant proteins alone, i.e. a “horizontal approach”, is limited. Reconstruction of protein history offers an extra level of perspective for determining what aspects of a protein are crucial to function and which are not. In particular, ASR allows for a direct analysis of which mutations gave a protein its functions, something that is rarely if ever possible using only extant proteins (Yokoyama, Yang, & Starmer 2008; Harms & Thornton 2010; Merkl & Sterner 2016). More generally, ASR can offer a glimpse at the evolutionary history of proteins, and the trends that define it (Bridgham *et al.* 2009; Voordeckers *et al.* 2012; Wheeler *et al.* 2016). ASR can even be useful in modern biotechnological applications as a protein engineering tool, since ancient enzymes

may have unique catalytic properties that are not found in any extant organism (Cole & Gaucher 2011; Whitfield *et al.* 2015).

ASR also offers invaluable insight into the molecular processes of evolution and has been instrumental in several discoveries about evolutionary history on a molecular level. For example, ASR was used to elucidate the evolutionary path of the steroid receptor family of proteins from a single promiscuous ancestor to a wide variety of proteins with high specificity (Eick *et al.* 2012). The same has been done for the evolution of visual colour pigments in vertebrates (Chinen, Matsumoto, & Kawamura 2005).

ASR was first conceived in 1963, although the first experiment using it was not performed until 1990 (Malcom *et al.* 1990; Hobbs *et al.* 2015; Joy *et al.* 2016). The earliest examples of ASR used maximum parsimony (MP) to generate their phylogenies (Merkl & Sterner 2016). However, MP is rarely used alone in modern inferences due to its limitations and biases. The most notable of these is the phenomenon known as long branch attraction, where highly divergent lineages are assumed to be more closely related than they really are. More modern techniques include neighbour joining, maximum likelihood, and Bayesian inference (Merkl & Sterner 2016). These are more complex statistical methods that require incorporation of a model of evolution, and with the right model they can provide a more accurate phylogeny when compared to MP. Within the past few years, it has been suggested that creating a phylogeny based on protein sequence alone is inadequate, and that sequence phylogenies should be combined with the phylogenies of the species they come from to improve accuracy (Szöllősi *et al.* 2014; Groussin *et al.* 2015).

While the evolutionary history of each protein is of course different, a few overarching trends have been suggested for protein evolution based on experiments done using ASR. The first and most well supported is the trend of decreasing thermostability over time. When looking at timescales of around a billion years or more, proteins resurrected through ASR tend to have high thermostability, which decreases over evolutionary time (Gaucher, Govindarajan, & Ganesh 2008; Perez-Jimenez *et al.* 2011; Hobbs *et al.* 2011; Akanuma *et al.* 2013; Risso *et al.* 2013; Butzin *et al.* 2013). This trend has been used as evidence that early life was by and large thermophilic (Di Giulio, 2003; Gaucher, Govindarajan, & Ganesh 2008;

Akanuma *et al.* 2013). Another trend, although less common, is that of decreasing catalytic activity in enzymes over time (Perez-Jimenez *et al.* 2011; Akanuma *et al.* 2013; Butzin *et al.* 2013). In terms of evolutionary history, ASR experiments have suggested that epistatic interactions are a major factor in how proteins evolve (Ortlund *et al.* 2007; Bridgham, Ortlund, & Thornton 2009). This hypothesis is supported by other phylogenetic works that did not use ASR (Phillips 2008; Lunzer, Golding, & Dean 2010).

It is possible that these trends are simply artefacts of ASR itself, and do not reflect reality. After all, ASR is entirely a statistical practice, and its findings cannot be empirically verified as no ancient ancestral proteins still exist. However, several studies lend support to the idea that resurrection of proteins through ASR offers a faithful reconstruction of the original (Hall 2006; Hanson-Smith, Kolaczkowski, & Thornton 2010; Akanuma *et al.* 2015), and although it does have biases (Krishnan *et al.* 2004; Williams *et al.* 2006), these do not seem to contribute towards the general trends. Despite the apparent broad accuracy of ASR, it is not a perfect process and it is unlikely that any resurrected protein will be exactly the same as the ancestor that it emulates.

## **1.2 The Use of ASR With LeuB Enzymes**

### **1.2.1 ANC1-4**

ASR was used to resurrect ancient ancestors of the *Bacillus* LeuB enzymes (Hobbs *et al.* 2011). In this study, four ancestors were generated, labelled ANC1-4. Each ancestor was older than the last, with ANC4 representing LeuB from the last common ancestor of all *Bacillus* species. The ancestors, as well as three contemporary LeuB enzymes (from a thermophilic, mesophilic, and psychrophilic *Bacillus* species), were characterized: The optimum temperatures and Michaelis-Menten constants were determined for each of the enzymes. These tests revealed, at least in part, the evolutionary pathway of *Bacillus* LeuB. The youngest ancestor, ANC1, was thermophilic, despite some of its contemporary descendants being psychrophiles. Going back further, ANC2 was mesophilic, while ANC3 and ANC4 were both thermophilic (ANC4 more so than ANC3).

This supports the widespread hypothesis that proteins around 1 billion years or older were highly thermophilic (with ANC4 simulating an approximately 950-million-year-old protein), but also shows that protein evolution is not a simple matter of linearly decreasing thermophily over time. As shown by the LeuB ancestors, lineages may develop and lose thermophilic properties multiple times throughout their evolutionary history. ANC4 also showed a substantial increase in efficiency when compared to contemporary thermophilic LeuB, and an increase in overall kinetic stability.

These findings present a puzzling question: Why would natural selection promote or allow a loss of stability and biochemical efficiency over evolutionary time? Do these traits incur a fitness cost?

Proteins are energetically very expensive to produce (Cox & Cook 2007; Edwards, Roberts, & Atwell 2012), and so highly stable proteins, with their relatively long half-lives, should conserve energy when compared to their less stable counterparts. Highly stable proteins are also less likely to form non-functional aggregates (Chi *et al.* 2003; DePristo, Weinreich, & Hartl, 2005), and are more able to accommodate novel mutations that could lead to new or improved function (Bloom *et al.* 2006; Tokuriki & Tawfik 2009; Dellus-Gur *et al.* 2013).

However, increased protein stability is not purely beneficial. Highly stable proteins are difficult to regulate, taking longer to degrade via cellular pathways and consuming much more ATP in the process (Kenniston *et al.* 2003). Studies have also observed an inverse relationship between protein stability and catalytic activity (Shoichet *et al.* 1995; Somero 1995), although this does not seem to be an issue for many resurrected enzymes, including the LeuB ancestors. Since most possible mutations to a protein are destabilising (Tokuriki *et al.* 2008), it is also possible that proteins are simply statistically likely to become less stable over time. Protein stability would then only be preserved if it is strongly favoured by natural selection, as is the case with thermophiles (Fields 2001).

Unlike protein stability, catalytic efficiency of enzymes has no known inherent downsides, and so at first it may seem that all enzymes should evolve towards catalytic perfection: The point at which the rate of an enzyme's reaction is limited only by the speed of diffusion (Albery, W. J. & Knowles, J. R., 1976). If the

observed trend of ancient enzymes having high catalytic efficiency is accurate, then this is clearly not the case. Indeed, most enzymes are nowhere near catalytic perfection, and only exhibit moderate catalytic efficiency (Bar-Evan *et al.* 2011).

This is likely because an enzyme's efficiency can only be relevant to natural selection if it is the slowest enzyme in its metabolic pathway. If it is not, then it doesn't matter how fast the enzyme is because the overall pathway will continue at the same rate. Furthermore, other factors may be selected for even at the cost of efficiency, slowly eroding an enzyme's catalytic efficiency until it becomes a problem for the organism (Newton, M. S., Arcus, V. L., & Patrick, W. M., 2015). This model of enzyme evolution may also explain why the trend of increased efficiency in ancient enzymes is less common than the trend of high stability: Enzyme efficiency is essentially cyclical, slowly degrading over evolutionary time until it becomes the slowest in its pathway. At this point mutations that increase efficiency become highly beneficial and will be selected for, causing efficiency to increase. If this cyclical model of enzyme evolution is correct, then it would be random chance what point of the cycle any given ancestor was at.

### **1.2.2 Fitness Experiments**

In 2015, Hobbs *et al.* transformed their previously constructed LeuB ancestors into *Escherichia coli*, to determine if their apparently favourable biochemical and physical properties conferred a fitness advantage over *E. coli* which had instead received contemporary *Bacillus* LeuB enzymes. They in fact determined the opposite: *E. coli* strains with the oldest LeuB ancestor, ANC4, struggled to grow on media with minimal nutrients, while those strains with contemporary and young ancestral LeuB thrived. This was despite ANC4 having a much higher catalytic efficiency and much greater kinetic and thermal stability than contemporary and young ancestral LeuB.

Further experimentation found no correlation between efficiency of LeuB and organismal fitness, nor between stability of LeuB and organismal fitness. However, a strong inverse correlation was found between the estimated age of an ancestral enzyme and the organismal fitness. Hobbs *et al.* tentatively concluded that the increasing evolutionary distance between older LeuB ancestors and the contemporary machinery of the *E. coli* caused epistatic discordance that incurred a

fitness cost. That is to say, the ancient enzyme was poorly adapted to work in the modern pathway. However, they also cautioned that their dataset was small, and that further research would be needed (Hobbs *et al.* 2015).

In addition, this hypothesis is problematic when considering that the experiment was performed with contemporary *E. coli*, which diverged from *Bacillus* long before the estimated age of any of the inferred ancestors. Therefore, all the inferred ancestors, as well as contemporary *Bacillus* LeuB, are equally related to the modern proteome of *E. coli*. An alternate hypothesis proposed by Hobbs *et al.* is that since ASR becomes less accurate the older an ancestor is, the dropping fitness with estimated age could simply be an artefact of ASR, and not reflective of reality.

Regardless of why, it is evident that despite showing apparently favourable biochemical properties, ancient LeuB ancestors impose a fitness cost upon modern *E. coli*. It is, at present, unknown whether this finding would be applicable to other ancient resurrected proteins. Despite the work of Hobbs *et al.*, it is still uncertain what causes this loss of fitness. Is it, as they suggested, a consequence of epistatic interactions? Or are these ancient enzymes generally inferior to their contemporary counterparts in ways that have not yet been elucidated? Is it simply due to limitations in the accuracy of ASR? The mechanism behind the poor *in vivo* properties of ancient LeuB ancestors is important to uncover, as it could reveal much about either enzyme evolution, the accuracy of ASR, or both.

### **1.2.3 Rec/LG and Rec/EX.**

In 2015, Groussin *et al.* used ASR to resurrect LeuB from the last common ancestor of the Firmicutes, the bacterial phylum to which *Bacillus* belongs. They used multiple models of evolution to infer multiple versions of this LeuB ancestor. Most ASR inferences only consider the sequence alignment of contemporary proteins (referred to as S-unaware trees). Groussin *et al.* attempted to reconcile this single gene phylogeny with a species level phylogeny (referred to as S-aware trees) which includes both protein and species information, giving much more context for the evolution of the contemporary proteins from their common ancestor.

The 2015 publication by Groussin *et al.* refers to two versions of LeuB from the last common ancestor of the Firmicutes. The first is LeuB<sub>S-unaw</sub>, which is based on an S-unaware LeuB phylogeny. The second is LeuB<sub>S-aw</sub>, which is based on an S-aware LeuB phylogeny. Both enzymes were inferred using the site heterogeneous EX\_EHO model of evolution. Although not mentioned in the final publication, another version of the ancestral LeuB was resurrected during the experiments of Groussin *et al.* This version was also inferred using an S-aware tree but used the site homogeneous LG model of evolution. This thesis deals with both LeuB<sub>S-aw</sub> and the unpublished enzyme and refers to them henceforth as Rec/EX and Rec/LG, respectively. Like many of the ancient LeuB ancestors characterised thus far, Rec/EX and Rec/LG show high thermostability (Both having a  $T_{opt}$  of 85 °C) and catalytic activity (With a  $K_{cat}$  of 181.2 s<sup>-1</sup> and 161.9 s<sup>-1</sup>, respectively) when compared to their contemporary counterparts. Although the kinetics of these enzymes have been characterised, no crystal structures, or even models of the structures, have been produced.

## **1.3 LeuB Structure and Function**

### **1.3.1 Leucine Biosynthesis**

Leucine is one of the twenty common amino acids found in the genetic code. Like all the common amino acids, it is used in the building practically all proteins (Garrett & Grisham 2005). As such, virtually all organisms must either take up or synthesise leucine to survive. In Bacteria, leucine biosynthesis is handled by the leucine operon, which is made up of four genes that code for three enzymes. Figure 1 depicts the biosynthesis of Leucine.

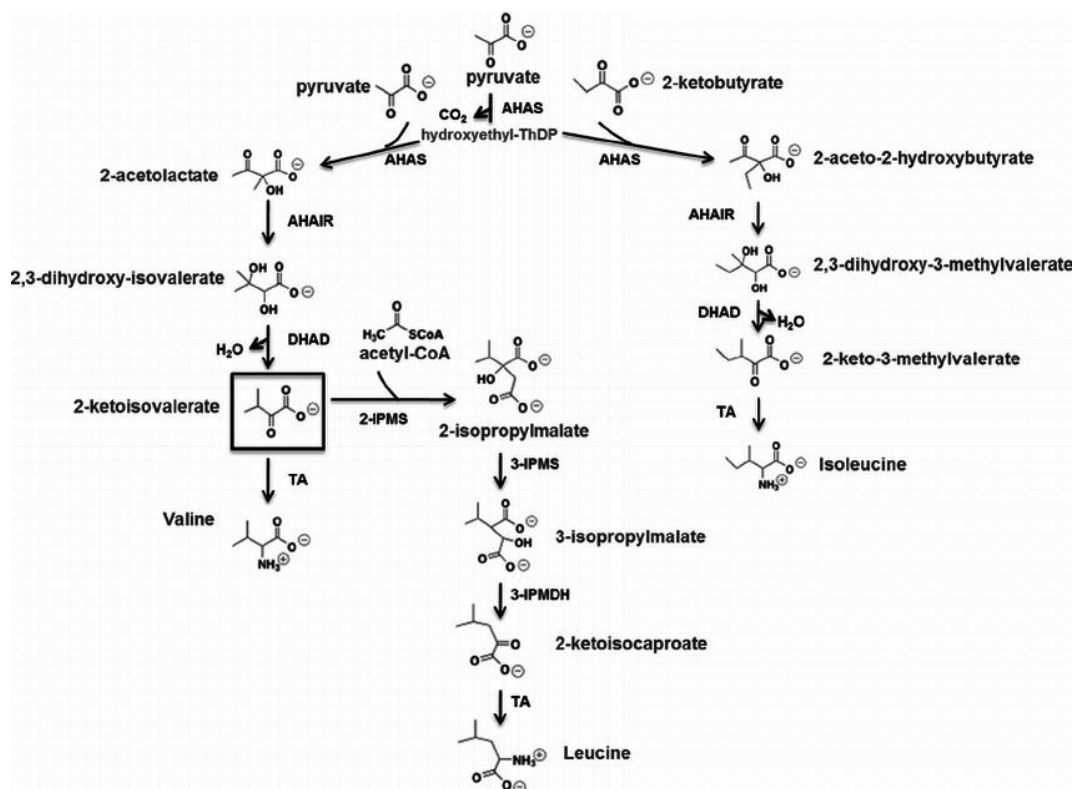


Figure 1: Schematic of the branched-chain amino acid (BCAA) biosynthesis pathway in *Ralstonia eutropha*, including the biosynthesis of leucine from 2-ketoisovalerate (Brigham et al., 2015).

The second enzyme in the leucine biosynthesis pathway is LeuB, also referred to in the literature as Isopropylmalate Dehydrogenase or IPMDH (sometimes the prefix 3- is used for both names, as is the case in Figure 1). This enzyme was first discovered in 1963 by Burns, Umbarger, and Gross. It acts on its two substrates, 3-isopropylmalate (IPM) and  $\text{NAD}^+$ , in the presence of a divalent cation, with  $\text{Mn}^{2+}$  being preferred (Wallon *et al.*, 1996). LeuB catalyses the transfer of a hydride ion from IPM to  $\text{NAD}^+$ , and the decarboxylation of IPM's keto acid to form  $\alpha$ -Ketoisocaproic acid (Pirrung, Han, & Nunn, 1994; Imada *et al.*, 1998).

### 1.3.2 Active Site of LeuB

The first crystal structure for LeuB was published in 1991 by Imada *et al.*, giving the structure of LeuB from *Thermus thermophilus*. This paper showed that LeuB consists of two domains of similar structure. These domains fold into a closed form where a hydrophobic pocket formed by both domains contributes to substrate binding and catalysis. While this hydrophobic pocket has a broad specificity towards alkylmalates, it does not bind to the very similar isocitrate (Miyazaki *et al.*

1993). Isocitrate has a carboxymethyl group on the  $\gamma$  carbon, whereas 3-isopropylmalate has an alkyl group in the same position (Figure 2).

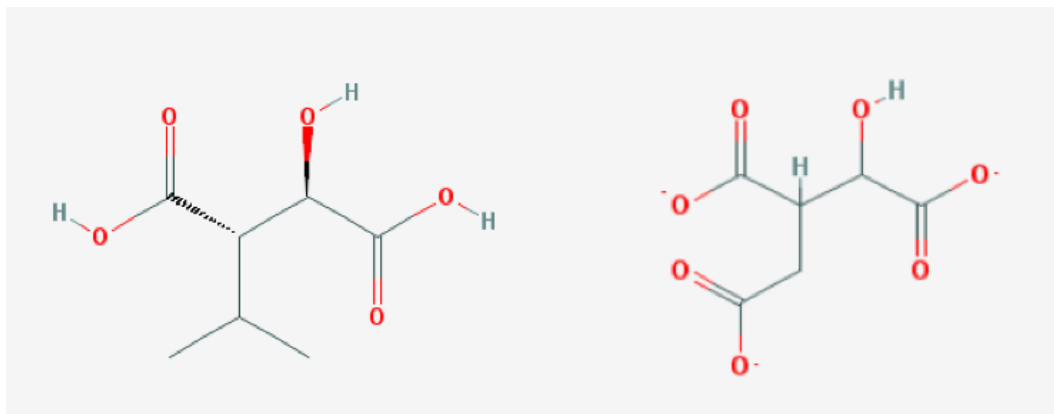


Figure 2: Isopropylmalate (left) and Isocitrate (right). The different groups attached to the  $\gamma$  carbon appear to be crucial in the substrate specificity of LeuB. Chemical structure images retrieved from <https://pubchem.ncbi.nlm.nih.gov> on 17.10.2017.

The inability of LeuB to bind to isocitrate despite its otherwise broad specificity strongly implies that the group attached to the  $\gamma$  carbon is crucial to the substrate recognition of LeuB. This hypothesis is supported by the 1998 paper of Imada *et al.*, who crystallized LeuB of *Thiobacillus ferrooxidans* in the presence of 3-isopropylmalate. Of the four amino acids that form the hydrophobic substrate binding pocket, they identified Glu88 as being essential to substrate recognition. In the active, closed form of LeuB, the carboxylic acid of the Glu88 sidechain sits in between the fork created by the  $\gamma$  alkyl group of 3-isopropylmalate. The close position of Glu88 to the substrate, and the extra turn in the helix responsible for the formation of the pocket, gives LeuB a long, narrow binding pocket relative to the very similar Isocitrate Dehydrogenase. It is this long and narrow binding pocket, in conjunction with the negatively charged Glu88, that excludes isocitrate from binding, while still allowing 3-isopropylmalate and alkylmalates to bind (Figure 3).

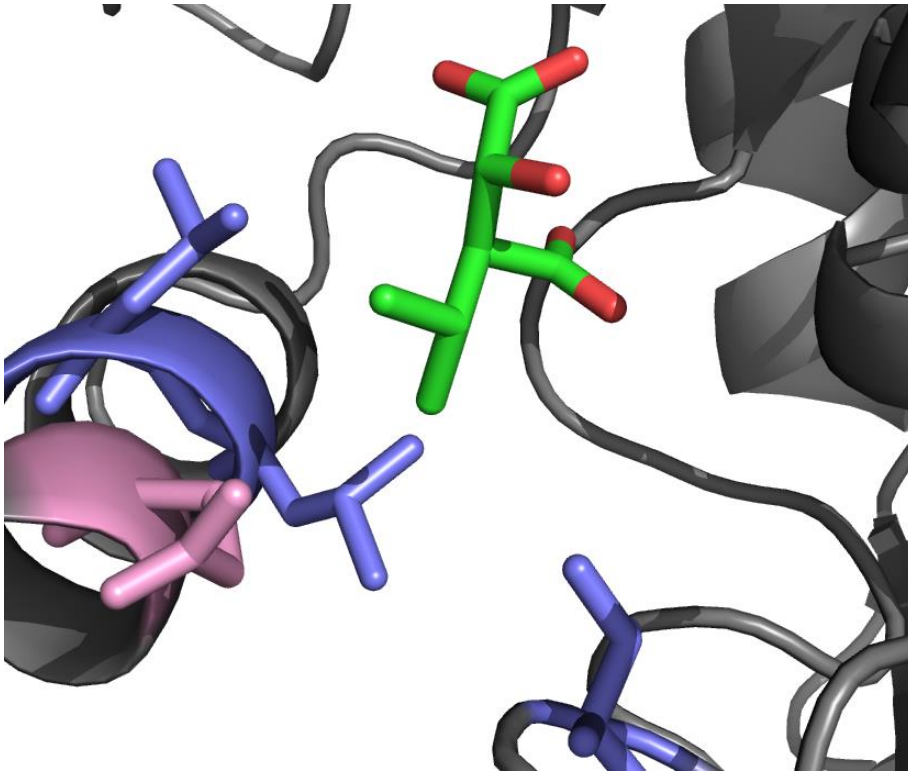


Figure 3: The substrate binding site of LeuB, complexed with IPM (green). Glu88 (pink) creates a negative charge at the mouth of the hydrophobic binding pocket which prevents binding of isocitrate. Leu91, Leu92, and Val193 (blue) all contribute to the formation of the hydrophobic binding pocket. Adapted from Imada et al. 1998.

An earlier work by Dean & Dvorak in 1995 further supports this hypothesis. Though not the primary focus of their paper, they found that mutants which replaced Glu87 (which, in *T. thermophilus*, sits at the opening of the hydrophobic binding pocket and so is homologous to the Glu88 in *T. ferrooxidans*) led to a reduction in substrate specificity. Despite the hypothesis that ancient ancestral enzymes were more promiscuous than their contemporary counterparts (Khersonsky & Tawfik 2010), resurrected ancestors of LeuB whose crystal structures have been solved all possess this key glutamic acid, and they appear to be just as specific as their contemporary counterparts (Hobbs *et al.* 2011, Prentice 2013).

### 1.3.3 Temperature and LeuB

LeuB enzymes are found in a wide variety of microbes. The organisms that possess LeuB can be thermophilic, even extremely so (Kagawa *et al.*, 1984). However, LeuB can also be found in mesophiles (Wallon *et al.*, 1997) and even psychrophiles (Svingor *et al.*, 2001). The temperatures across which these organisms can grow ranges from -1.5 °C to 80 °C (Wiebe, Sheldon, & Pomeroy, 1991; Beffa *et al.*,

1996). This vast temperature range implies a massive amount of temperature adaptations across different LeuB enzymes.

Many experiments have been done with LeuB to uncover the structural features that confer thermal stability. Wallon *et al.* in 1997 compared the crystal structures of LeuB from the mesophiles *E. coli* and *Salmonella typhimurium* to that of the extreme thermophile *T. thermophilus*. The main structural differences that they identified as contributing to thermostability were more ion pairs and hydrogen bonds, a tighter association of subunits due to a more hydrophobic and relatively larger interface, and a higher proportion of the highly rigid amino acid proline. The individual contributions of these features could not be identified. However, the stability offered by the increased hydrophobic interaction of the subunit interface had previously been experimentally verified by Kirino *et al.* in 1994. Kirino *et al.* mutated *E. coli* LeuB to increase the hydrophobicity of the interface, and did the opposite with *T. thermophilus* LeuB. They found that the *E. coli* mutant was more thermostable, and the *T. thermophilus* one was less thermostable. Németh *et al.* in 2000 further demonstrated the importance of ion pairs in LeuB thermal stability with a mirror mutation experiment. This experiment eliminated one ion cluster in *T. thermophilus* LeuB and introduced a homologous ion cluster in the LeuB of *E. coli*. The mutants were unambiguously less and more thermostable, respectively, than their wildtype counterparts.

## **1.4 Bacterial Evolution Experiments**

### **1.4.1 A Brief Overview**

Bacteria have long been used as models to observe and experiment with the processes of evolution (O'Malley 2017). Early research in the area was largely unconcerned with bacteria themselves, but saw the benefit in using the relatively simple and much easier to work with single celled organisms to help explain underlying concepts of evolution that could also be applied to plants and animals (O'Malley 2017).

Not just limited to serving as a model for complex organisms, bacterial evolution experiments are often used to elucidate evolutionary phenomena that are unique to bacteria themselves (such as the works of Lenski 1998; Björkman *et al.* 2000; Lázár

*et al.* 2013). Bacteria are also used to study molecular evolution. This focuses on changes to single molecules such as genes or proteins, rather than entire organisms or populations (Papadopoulos *et al.* 1999; Woods *et al.* 2006; Paterson *et al.* 2010).

#### **1.4.2 Evolution in *Bacillus subtilis***

*B. subtilis* is a rod shaped, gram positive, endospore forming species of bacteria. It has been extensively studied and is considered a model organism for laboratory experimentation (Mäder *et al.* 2011). The largest evolution experiment done to date with *B. subtilis* is a 6,000 generation experiment first reported on by Maughan *et al.* in 2006. In this experiment, 5 lines were evolved in conditions intended to strongly select for sporulation, while 5 other lines were evolved in relaxed conditions in which the ability to sporulate offered no benefit.

Under the relaxed conditions, two strains developed a severely reduced ability to sporulate, while three lines lost the ability entirely. Because sporulation is a very complex process relying on the coordinated efforts of 210 genes to carry out, there is plenty of room for random mutations to shut down sporulation in an environment where the ability to sporulate is a neutral trait (referred to by Maughan *et al.* 2007 as mutational degradation, or MD). However, it is also a very energetically expensive and time-consuming process, and so could be subject to negative selection. In 2007, Maughan *et al.* found significant evidence for negative selection in only one of the five strains in which sporulation was reduced or eliminated. This indicates that mutational degradation is the primary cause for loss of sporulation in experimental populations of *B. subtilis*.

Maughan & Nicholson reported in 2011 that four of the five strains grown in spore repressing media adopted a novel colony morphology which they dubbed the Small Colony Variant (SCV). This morphology was defined by the small distinct colonies formed when the strains were grown on agar plates. Other phenotypic traits were noted amongst SCV strains, but none occurred in all four. Because the SCV emerged in four independent strains of bacteria, Maughan & Nicholson hypothesised that either the SCV or a phenotype strongly correlated with it was beneficial to growth in spore repressing media.

## 1.5 The Evolution of Rec/LG and Rec/EX

Dr. Emma Andrews of the Proteins and Microbes laboratory at the University of Waikato carried out an evolution experiment to compare the evolutionary trajectories of native *B. subtilis* W168 with replacement mutant strains containing the genes for Rec/EX and Rec/LG in place of their native LeuB. Extensive efforts were also made to replace the native LeuB gene of *B. subtilis* with other inferred ancestors, such as ANC4, but as of yet only Rec/EX and Rec/LG mutants have been successfully created. The methodology of the evolution experiment was based on the 6,000-generation *B. subtilis* evolution experiment (see Materials and Methods of Maughan *et al.* 2006), although with a different medium to ensure the synthesis of leucine via the leucine biosynthetic pathway (see appendix). Initially, the spore inducing media and heat shock process used by Maughan *et al.* was applied to the evolution experiment to prevent loss of sporulation. However, this led to the extinction of every cell line. In parallel, a medium adapted from the spore repressing medium used by Maughan *et al.* was used. Each strain was run in triplicate for 400 generations, with a glycerol stock of each culture being taken every 50 generations.

The purpose of this thesis project was to analyse the genetic differences in the 9 cultures as they evolved over 400 generations. In particular, the focus for this project was any evolution that may have affected the LeuB enzyme, be it through mutations to the *leuB* gene, or changes in its regulatory regions. If significant changes to the *leuB* gene were found, differences in enzyme kinetics and possibly structure would be analysed.

## Structure of Rec/LG and Rec/EX

---

### 2.1 Introduction

The crystal structures of many different LeuB enzymes have been solved, including several resurrected ancestors (Imada *et al.* 1991; Wallon *et al.* 1997; Imada *et al.* 1998; Graczer *et al.* 2011; Hobbs *et al.* 2011; Prentice 2013). These crystal structures have helped to elucidate much about the structural elements behind the substrate specificity, activity, and stability of LeuB. Rec/LG and Rec/EX both show impressive catalytic activity and stability, but to date their crystal structures have not been solved. The structures of these enzymes could be valuable pieces in the ongoing efforts to determine exactly how differences between enzyme structures affect their kinetic properties. Furthermore, they could be used as reference points when analysing the evolved Rec/LG and Rec/Rec/EX to determine if significant structural changes occurred over the course of the evolution experiment.

### 2.2 Methods

#### 2.2.1 Protein Expression

The genetic sequences for Rec/LG and Rec/EX were cloned into pPROEX plasmids and transformed into *E. coli* (Groussin *et al.* 2015). Glycerol stocks of these transformants were kept at -70 °C. For expression, initially samples of these stocks were streaked out on LB agar with ampicillin (1000:1) and incubated at 37 °C overnight. Swabs from these colonies were used to inoculate 10 mL of LB broth with ampicillin (1000:1) starter cultures, and these starter cultures were incubated at 37 °C and 200 rpm overnight. Each starter culture was added to 1 L of LB broth with ampicillin (1000:1), and these cultures were incubated at 37 °C and 200 rpm. The OD<sub>600</sub> for these cultures was monitored until it reached an absorbance between 0.4 and 0.6. At this point, 1 mL of 0.75 M IPTG was added to induce protein expression. After induction, cultures were incubated overnight at 37 °C and 200 rpm. The cells were then pelleted and stored at -70 °C.

A series of experiments were carried out to streamline this process. The new method for protein expression started with direct inoculation of 10 mL LB broth with

ampicillin (1000:1) starter cultures with 10  $\mu$ L of the glycerol stocks of Rec/LG or Rec/EX. These starter cultures were incubated at 37 °C and 200 rpm overnight. Each starter culture was added to 1 L of LB broth with ampicillin (1000:1). One mL of 0.75 M IPTG was immediately added to induce protein expression, and cultures were incubated overnight at 37 °C and 200 rpm. The cells were then pelleted and stored at -70 °C.

### **2.2.2 Protein Purification**

Cell pellets containing the relevant protein were resuspended in a 50 mM sodium phosphate buffer at pH 8 with 300 mM sodium chloride and 20 mM imadazole (nickel buffer A). The resuspended cells were lysed using a Sonicator XL2020 (Misonix, Farmingdale, NY, USA) with a fine tip at setting 5 for 6x 20s bursts, with 30s on ice between each burst. Cell debris was then pelleted at 19,650 rcf for 20 min at 4 °C. Supernatant was filtered through 1.2, 0.45, and 0.2  $\mu$ m filters and loaded into a HisTrap HP Nickel Column (GE Healthcare, Chicago, IL, USA). The nickel purification graduated from nickel buffer A to a 50 mM sodium phosphate buffer at pH 8 with 300 mM sodium chloride and 1 M imadazole (nickel buffer B) over 50 mL using an ÄKTA Purifier (GE Healthcare, Chicago, IL, USA).

The nickel purification fractions containing protein were combined in a 10,000 MWCO concentrator and centrifuged at 3480 rcf in 10 min intervals until a volume of approximately 750  $\mu$ L was reached. This concentrated solution was put through size exclusion using either a Superdex 200 10/300 (GE Healthcare, Chicago, IL, USA) or a HiLoad 16/60 Superdex 200 (GE Healthcare) column as available. at first, size exclusion was performed using a 20 mM potassium phosphate buffer at pH 7.6. Due to problems with the production of salt crystals in crystal screens, and the formation of a white precipitate in the assay buffer which contained manganese, this was switched to a 20 mM HEPES buffer.

Protein concentration was measured using a NanoDrop 2000 (Thermo Fisher Scientific, Waltham, MA, USA), considering the extinction coefficient calculated by ProtParam based on the protein's amino acid sequence.

### 2.2.3 Robotic Crystallisation Screens

To grow crystals of Rec/LG and Rec/EX, a wide variety of possible crystallisation conditions were sampled via robotic screenings. The screening conditions used were SaltRx 1, SaltRx 2, PEGRx 1, PEGRx 2, Crystal Screen, Crystal Screen 2, and Index (Hampton Research, Aliso Viejo, CA, USA). For Rec/LG, these screening conditions were used with 3 different protein concentrations (9 mg/mL, 35 mg/mL, and 50 mg/mL). For Rec/EX, 3 different protein concentrations were used (4 mg/mL, 43 mg/mL, and 56 mg/mL). Since LeuB undergoes a large conformational change when bound to IPM (Imada *et al.* 1998), an additional protein condition was created by adding 4 mM IPM to the protein (25 mg/mL) prior to creating the screen. Sitting drops with a 1:1 ratio of protein to mother liquor were set up for each condition using a mosquito crystallisation robot (TTP Labtech, Melbourn, United Kingdom).

### 2.2.4 Fine Screens

Robot screen conditions which produced crystals were used as the basis for fine screens. All fine screens used the hanging drop method with a 1:1 ratio of protein to mother liquor. Variables such as pH and concentrations of additives were altered in increments to replicate and optimise crystal growth. All in all, 11 fine screens were created for Rec/LG, while 12 were created for Rec/Rec/EX (see appendix).

### 2.2.5 Structure Modelling and Analysis

The amino acid sequences of Rec/LG and Rec/EX were submitted to SWISS-MODEL (Arnold *et al.* 2006; Geux, Peitsch, & Schwede 2009; Kiefer *et al.* 2009; Biasini *et al.* 2014). SWISS-MODEL predicted the 3D structure of Rec/LG and Rec/EX based on their amino acid sequences, using ANC4 (as published by Hobbs *et al.* 2011) as a template. Crystal structures of *T. thermophilus* LeuB bound to NADH (Graczer *et al.* 2011) and *T. ferrooxidans* LeuB bound to IPM (Imada *et al.* 1997) were used to aid the analysis of the model structures. These two crystal structures were aligned to the crystal structure of ANC4 and the models of Rec/LG and Rec/EX to simulate the position of the substrates within these enzymes.

## 2.3 Results and Discussion

### 2.3.1 Crystallisation of Rec/LG and Rec/EX

Both Rec/LG and Rec/EX were successfully overexpressed, purified, and crystallised several times. Figure 4 shows a selection of some of the best (largest, with the most well-defined edges and regular shape) crystals of both Rec/LG and Rec/EX.

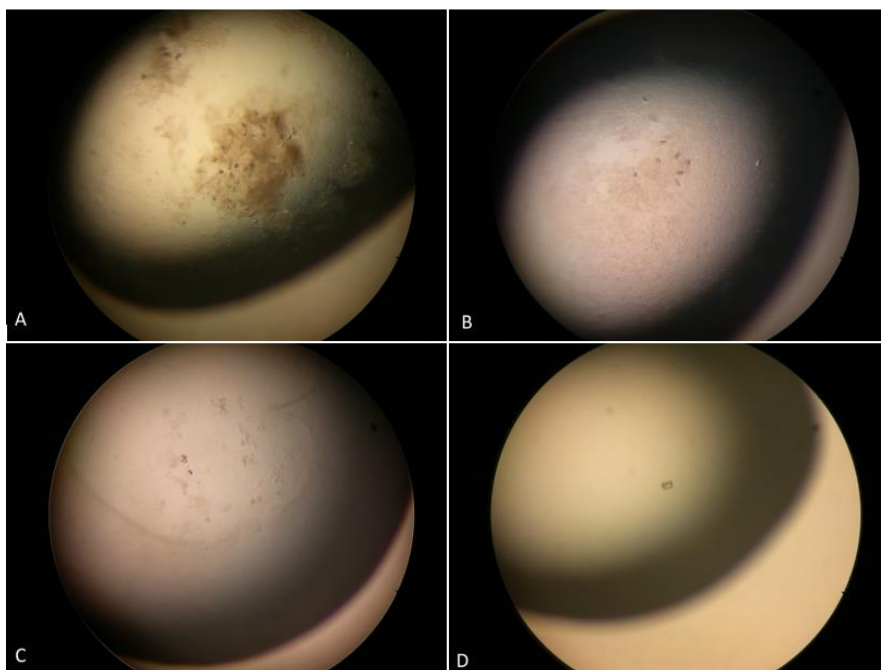


Figure 4: Pictures of protein crystals of Rec/LG and Rec/EX. See appendix for crystallisation conditions.

Despite trying a total of 1,416 different conditions for Rec/LG and 1,824 for Rec/EX, not a single protein crystal of sufficient quality for X-ray diffraction was obtained. The primary problem was size, with even the largest crystals being too small to successfully loop. The only crystals that could be looped were shown to be salt crystals by X-ray diffraction on a SuperNova Single Crystal Diffractometer (Agilent Technologies, Santa Clara, CA, USA).

### 2.3.2 Structure Models for Rec/LG and Rec/EX.

SWISS-MODEL was able to successfully generate models of the 3D structure for both Rec/LG and Rec/EX. These structural models were analysed and compared to existing LeuB crystal structures to determine whether the models could explain any of the kinetic traits of Rec/LG and Rec/EX.

SWISS-MODEL primarily uses a statistic called Qualitative Model Energy Analysis (QMEAN) to assess the overall quality of a model. This composite statistic looks at the torsion angles between amino acids, the distance between C $\beta$  atoms, and the degree to which hydrophobic amino acids are buried within the structure. The overall QMEAN score for the model is calculated based on how close these factors are to those of experimental structures of a similar size. The model of Rec/LG was assigned a QMEAN score of -1.68, while Rec/EX was assigned a score of -1.87. SWISS-MODEL defines models with scores lower than -4.0 as poor quality. SWISS-MODEL also uses a statistic called Global Model Quality Estimation (GMQE). This statistic is based on the alignment of the model's sequence to its template's sequence, but also takes into account the QMEAN of a model. Each model is assigned a GMQE score between 0 and 1, with higher numbers indicating a more reliable model. The model of Rec/LG was assigned a GMQE score of 0.78, while the model of Rec/EX was assigned a GMQE score of 0.76. Based on these scores, the overall models of Rec/LG and Rec/EX are likely to be accurate. However, SWISS-MODEL also assigns a local quality estimate between 0 and 1 to each residue based on the same factors, with higher numbers indicating higher quality. Figure 5 illustrates this local quality for Rec/LG and Rec/EX using the B factor putty function of PyMOL, since SWISS-MODEL uses this local quality estimate in lieu of B factor values. Despite the overall models being of reasonably high quality, some areas of each model are unreliable.

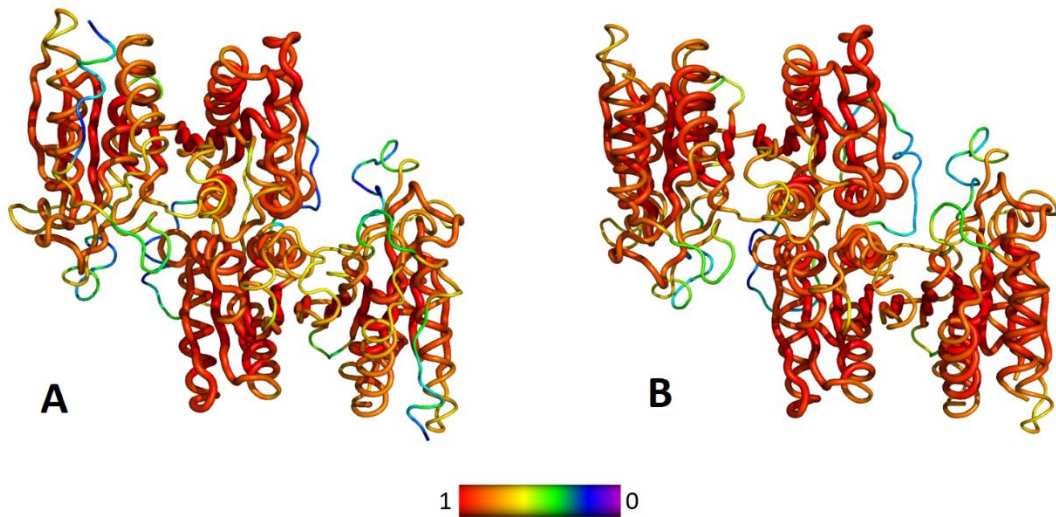


Figure 5: B factor putty cartoons of A: The Rec/LG model and B: The Rec/EX model, using SWISS-MODEL's local quality estimate in place of B factor values. Higher numbers, towards the red end of the colour spectrum, indicate a higher quality.

Predictably, the models of Rec/LG and Rec/EX were very similar to the crystal structure of ANC4, which was used by SWISS MODEL as the template for the models. Despite ANC4 having a moderate  $K_M^{(NAD)}$  much lower than either Rec/LG or Rec/Rec/EX (1.0 for ANC4, 3.6 for Rec/LG, and 6.5 for Rec/EX), there was no obvious differences between the NAD binding sites of ANC4 and the models. Figure 6 shows the close similarities between the NAD binding sites of Rec/LG, Rec/EX, and ANC4. All the residues that appear to interact with NAD are identical in Rec/LG and Rec/EX, with only a single difference between these and ANC4. The position of Leu259 in ANC4 is instead occupied by Ile258 in the models of Rec/LG and Rec/EX. This change slightly alters the geometry of the binding site, but not to a degree that would explain the huge differences in  $K_M^{(NAD)}$  between the enzymes. Without the true crystal structures of Rec/LG and Rec/EX, it is impossible to tell whether this high similarity is an artefact of the modelling process. It could be due to the ancestors all being closely related, or perhaps even an artefact of ASR.

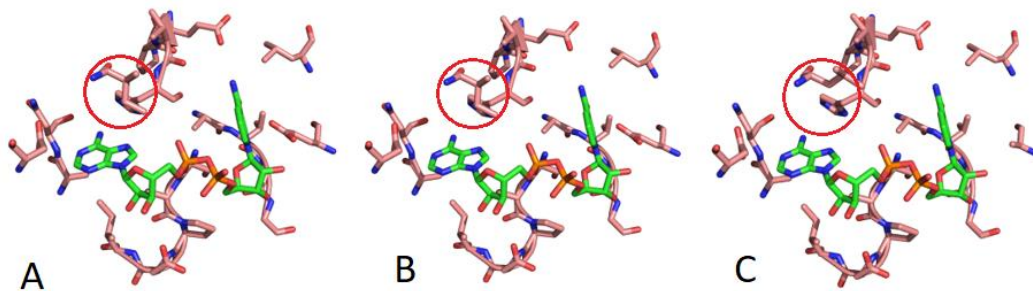


Figure 6: The near identical NAD binding sites of A: Rec/LG. B: Rec/EX. C: ANC4. The only residue not conserved between all three is circled in red. Position of NADH adapted from Graczer et al. 2011. Structure of ANC4 adapted from Hobbs et al. 2011. Note that the glutamic acid on the far right in A and B is also present in C, but it has not been properly represented in the crystal structure.

The rest of the enzymes' active sites are similarly conserved, illustrated by figure 6. Despite ANC4 having a  $K_{cat}$  double that of Rec/EX, and more than double that of Rec/LG, the active sites are very similar. Aside from the single substitution mentioned above, there are only slight differences in the position of residues within the binding site, the largest of which is Tyr140. Figure 7 illustrates both the high degree of similarity and slight differences between active sites.

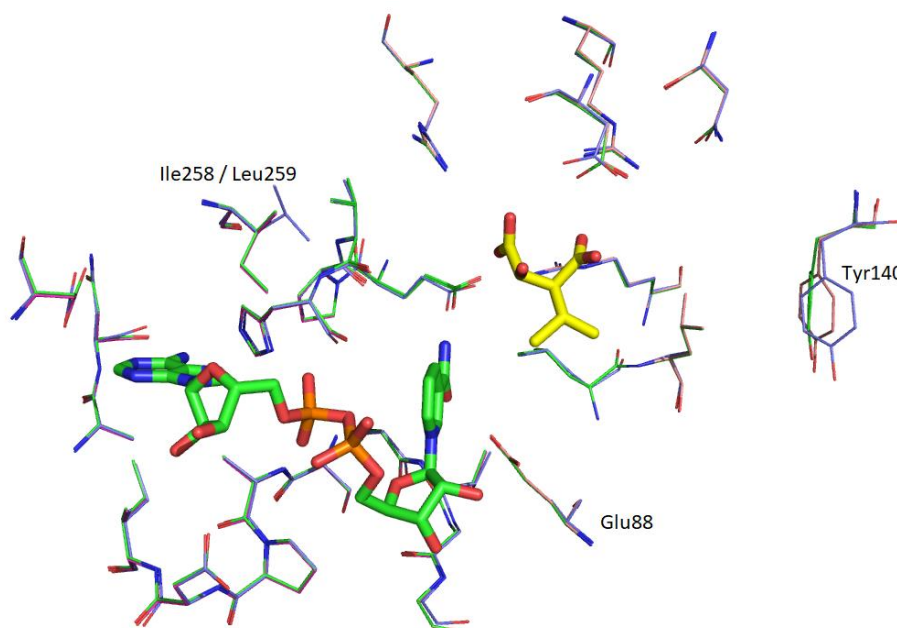


Figure 7: The active sites of Rec/LG (pink Carbons), Rec/EX (green Carbons), and ANC4 (blue Carbons) overlapping and shown as lines. Position of NADH (green Carbons) adapted from Graczer et al. 2011. Position of IPM (yellow Carbons) adapted from Imada et al. 1997. Structure of ANC4 adapted from Hobbs et al. 2011.

Overall, the models of Rec/LG and Rec/EX did not offer significant insight into the structural basis of their impressive kinetic properties. This could be due to the modelling method used overestimating the similarity between Rec/LG, Rec/EX,

and ANC4. However, the links between structure and function in proteins have not been completely solved. It is possible that the models of Rec/LG and Rec/EX are accurate representations of their true structure, and that their kinetic properties are tied to structural elements that are not yet understood.

# 3

## Genetics of the Evolution Experiment

---

### 3.1 Introduction

The primary purpose of this thesis was to analyse the evolution of 9 cultures of *B. subtilis*, with a focus on any changes that might have occurred to the *leuB* gene or regulatory regions. Of further interest were any potential differences between how the contemporary W168 *leuB* changed, and how the ancestral Rec/LG and Rec/EX *leuB* changed. To perform this analysis, genomic DNA extraction was attempted from a total of 30 samples of *B. subtilis*. Three of these were the parent strains, each of which was used in triplicate to create the 9 cultures. The remaining 27 stocks were the 9 cultures at 3 time points of evolution: Generation 54, generation 199, and generation 298. High quality, whole genomic DNA extraction and PCR amplification of just the *leuB* gene were both attempted.

### 3.2 Methods and Method Development

#### 3.2.1 Genomic DNA Extraction

Dr. Andrews started the work of optimising genomic DNA extraction from the 30 *B. subtilis* samples. She developed a method in collaboration with Dr. Ray Cursons of the Molecular Genetics lab at the University of Waikato. This method started with resuspending sample cells in 100  $\mu\text{L}$  of TE buffer (10 mM Tris and 1 mM EDTA, pH 8) in a 1.5 mL centrifuge tube. To this, 10  $\mu\text{L}$  of 100 mg/mL lysozyme was added. The solution was incubated at 37  $^{\circ}\text{C}$  for 30 minutes in a thermomixer at 750 rpm. After incubation, 350  $\mu\text{L}$  of lysis solution (100 mM Tris pH 8, 40 mM EDTA, 2 mM SDS, 10 mM NaCl) was added and the solution was mixed by inverting. To this, 10  $\mu\text{L}$  of 60 mg/mL proteinase K was added, and the solution was incubated at 65  $^{\circ}\text{C}$  for 30 minutes in a thermomixer at 750 rpm. Next, 350  $\mu\text{L}$  of 5 M  $\text{LiCl}_2$  was added. The solution was mixed via shaking. To this, 80  $\mu\text{L}$  of 270 mM cetrimonium bromide (CTAB) was added, and the solution was incubated at 65  $^{\circ}\text{C}$  for 30 minutes in a thermomixer at 750 rpm. Around 550  $\mu\text{L}$  of chloroform was added. The solution was mixed by shaking for 20 seconds and then centrifuged

at 15,700 rcf for 10 minutes at room temperature. The aqueous phase was transferred to a new tube. An equal volume of IPA was added to the solution, which was then incubated at -20 °C for 15 minutes. The solution was then centrifuged at 15,700 rcf for 15 minutes at room temperature. The supernatant was removed and discarded, and the pellet was washed with 1 mL of 70 % ethanol. The solution was centrifuged at 15,700 rcf for 5 minutes at room temperature. The supernatant was removed, and the pellet was allowed to air dry. After drying, the pellet was resuspended in 50 µL TE.

Despite extensive attempts at optimising, the developed method was insufficient for extracting enough DNA of high enough quality for whole genome sequencing. The primary problem was the presence of degraded DNA and / or RNA contamination. Attempts to remedy this caused overall yields to plummet to unusable levels. Due to going on maternity leave, Dr. Emma Andrews was unable to continue with the work, which was picked up by the author.

Further attempts were made to optimise yield, purity, and minimise DNA degradation. Partial success was found with a method similar to the original, but including additional purification steps. After proteinase K incubation, 50 µL of 5 M NaC<sub>2</sub>H<sub>3</sub>O<sub>2</sub> was added to the solution. To this, about 500 µL of phenol chloroform was added. The solution was mixed by shaking for 15 seconds, then centrifuged at 15,700 rcf for 10 minutes at room temperature. The aqueous phase was transferred to a new tube, to which 50 µL of 5 M NaCl<sub>2</sub> was added. About 500 µL of chloroform was added, and hereon the method is the same as the one outlined above. As a proof of concept, 10 µL of 20 mg/mL RNase A was added to the samples obtained through this method in an attempt to clear up RNA contamination.

The method which yielded the best results (defined by a combination of yield, purity, and minimal DNA degradation) started with resuspending sample cells in 100 µL of TE buffer in a 1.5 mL centrifuge tube. To this, 10 µL of 100 mg/mL lysozyme was added. The solution was incubated at 37 °C for 30 minutes in a thermomixer at 750 rpm. After incubation, 350 µL of lysis solution (100 mM Tris pH 8, 40 mM EDTA, 2 mM SDS, 10 mM NaCl) was added and the solution was mixed by inverting. To this, 10 µL of 60 mg/mL proteinase K was added, and the solution

was incubated at 65 °C for 30 minutes in a thermomixer at 750 rpm. Next, 350 µL of 5 M LiCl<sub>2</sub> was added. The solution was mixed via shaking. To this, 80 µL of 270 mM CTAB was added, and the solution was incubated at 65 °C for 30 minutes in a thermomixer at 750 rpm. About 550 µL of chloroform was added. The solution was mixed by shaking for 20 seconds and then centrifuged at 15,700 rcf for 10 minutes at room temperature. The aqueous phase was transferred to a new tube. To this, 20 µL of 20 mg/mL RNase A was added. The solution was incubated at 37 °C for 30 minutes. About 550 µL of chloroform was added. The solution was mixed by shaking for 20 seconds and then centrifuged at 15,700 rcf for 10 minutes at room temperature. The aqueous phase was transferred to a new tube. An equal volume of IPA was added to the solution, which was incubated at -20 °C for 60 minutes. The solution was then centrifuged at 15,700 rcf for 15 minutes at room temperature. The supernatant was removed and discarded, and the pellet was washed with 1 mL of 70% ethanol. The solution was centrifuged at 15,700 rcf for 5 minutes at room temperature. The supernatant was removed, and the pellet was allowed to air dry. After drying, the pellet was resuspended in 50 µL TE.

### 3.2.2 PCR Amplification of the *LeuB* Gene

The initial method used to perform PCR on the evolved samples was previously developed by Dr. Andrews. The master mix used consisted of 1.5 µL 10x Pfx buffer (Thermo Fisher Scientific), 10 mM dNTPs, 50 mM MgSO<sub>4</sub>, 1.5 µL of forward and reverse primers, 0.25 µL of Platinum Pfx (Thermo Fisher Scientific), and 7.5 µL of ultrapure water for each reaction. To obtain the template for the reaction, cell scrapings were resuspended in 20 µL of TE. The resuspended cells were incubated at 95 °C for 10 minutes and then briefly spun down in a PCR tube minispin. To each reaction, 2 µL of the solution was added. The PCR reaction started with a 2 min incubation at 95 °C. It then went through 30 cycles of the following: 95 °C for 15 seconds; 55 °C for 30 seconds; 68 °C for 45 seconds. Finally, the reaction was left at 68 °C for 5 minutes. This method is hereafter referred to as Pfx-culture.

When the above method was developed, the primers used were 10 base pairs upstream and downstream of the *leuB* gene. However, the primers originally used in this project were designed to start 20 base pairs upstream and end downstream

of the *leuB* gene, so that the poor quality reads common at the start and end of sequencing would not affect data for the gene. Unfortunately, an error was made in ordering the primers that caused them to be non-functional. Even after remedying this error, the PCR reaction conditions outlined above did not work with the new set of primers. Even using the original set of primers positioned at the beginning and end of *leuB*, using the original reaction conditions only worked on some of the evolved samples. Any successful PCR products were kept, and multiple different methods and slight variations on said methods were tried to get products from as many of the 30 samples as possible, as detailed below.

The second successful method (Pfx-glycerol) was the same as the original, except substituting 5  $\mu$ L of the glycerol stock of the sample for the cell scrapings used in the first step. A third (HF-glycerol) was a HOT FIREPol (Solis BioDyne, Tartu, Estonia) based reaction. The master mix for this reaction was made up of 5  $\mu$ L 10x B1 buffer (Solis BioDyne), 4  $\mu$ L 25 mM MgCl<sub>2</sub>, 1.25  $\mu$ L 10 mM dNTPs, 36.5  $\mu$ L ultrapure water, 1.5  $\mu$ L of 10  $\mu$ M forward and reverse primers, and 0.25  $\mu$ L of HOT FIREPol for each reaction. To supply the template, 2  $\mu$ L of glycerol stock was added directly to the master mix. The PCR reaction started with a 15 min incubation at 95 °C. It then went through 10 cycles of the following: 95 °C for 20 seconds; 67 °C for 20 seconds, dropping by 1 °C each cycle; 72 °C for 20 seconds. After those 10 cycles, it went through 30 cycles of the following: 95 °C for 20 seconds; 57 °C for 20 seconds; 72 °C for 20 seconds. Finally, the reaction was left at 68 °C for 5 minutes.

The PCR products produced by these methods were cleaned up using the High Pure PCR Product Purification Kit Version 16 (Roche Applied Science, Penzberg, Germany) according to the manufacturer's instructions.

### **3.2.3 DNA Quality**

The yield and purity of genomic DNA and PCR products was measured using a NanoDrop 2000 (Thermo Fisher Scientific). Presence or absence of PCR products and / or degraded DNA were observed via gel electrophoresis using 1% agarose gels stained with 1x SYBR Safe DNA Gel Stain (Invitrogen, Carlsbad, CA, USA).

All such gels were run alongside a 1 Kb Plus ladder (Invitrogen) and imaged using an Omega Lum<sup>TM</sup> G Imaging System (Aplegen, San Francisco, CA, USA).

### 3.3 Results

#### 3.3.1 Genomic DNA Extraction

Initial DNA extraction attempts resulted in both excessive degradation of DNA, and possible RNA contamination. 260/280 nm ratios of 2.0 – 2.1, like those shown in table 1, are indicative of RNA. Pure DNA has a 260/280 nm ratio of 1.8. However, these values are by no means absolute. Given that no visible bands of RNA could be seen in agarose gels (such as the one shown in figure 8), it is uncertain whether RNA contamination was a significant issue.

Table 1: One example of yield and purity of genomic DNA extracted from the parents of W168, Rec/Rec/LG, and Rec/EX using the original method.

Sample	DNA Concentration (ng/ $\mu$ L)	260/280	260/230
W168 Parent	446.4	2.12	2.22
Rec/LG Parent	811.5	2.04	2.25
Rec/EX parent	441.9	2.04	1.86

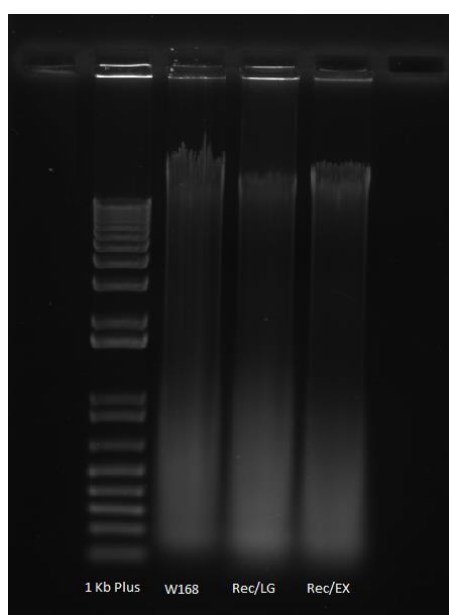


Figure 8: 1% agarose gel of genomic DNA extracted from the parents of W168, Rec/LG, and Rec/EX using the original method.

The phenol chloroform based method had major problems with 260/230 contamination. The addition of RNase A significantly improved the smearing visible on the agarose gels, as illustrated by figure 9. Predictably, the addition of RNase A to a completed DNA extraction pushed the 260/280 ratios to unacceptable levels, shown in table 2 alongside the 260/230 issues. These issues with purity made the samples unsuitable for whole genome sequencing.

Table 2: Yield and purity of genomic DNA extracted from Gen54 W168 samples, using the phenol chloroform based method.

Sample	DNA Concentration (ng/ $\mu$ L)	260/280	260/230
54 W168 A	342.9	1.40	0.92
54 W168 B	145.3	0.96	0.20
54 W168 C	161.2	0.87	0.14

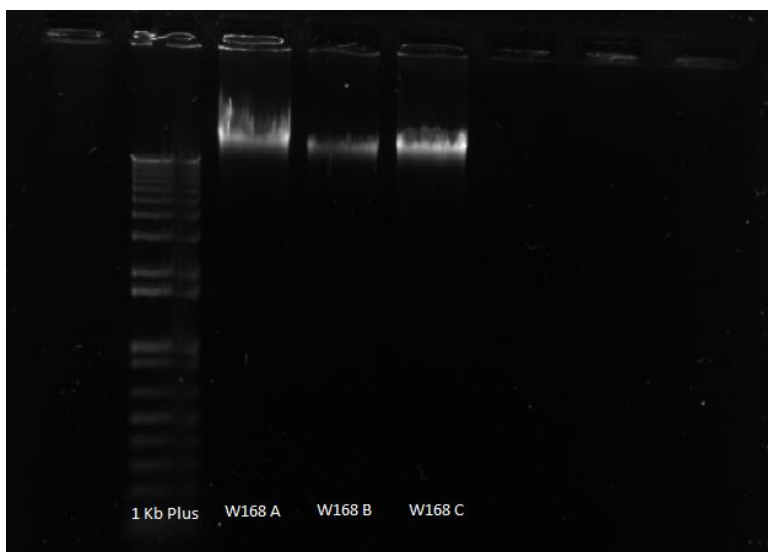


Figure 9: 1% agarose gel of genomic DNA extracted from Gen54 W168 samples, using the phenol chloroform based method.

The optimised genomic DNA extraction method produced DNA of sufficient quality for whole genome sequencing. It was used to extract DNA from the W168, Rec/LG, and Rec/EX parents. Table 3 shows that the 260/280 nm ratios are more in line with what is expected from pure DNA, while figure 10 shows the marked improvements to the problem of DNA degradation.

Table 3: Yield and purity of genomic DNA extracted from the parents of W168, Rec/LG, and Rec/EX using the optimised method.

Sample	DNA Concentration (ng/ $\mu$ L)	260/280	260/230
W168 Parent	162.8	1.93	1.99
Rec/LG Parent	506.8	1.88	1.95
Rec/EX parent	1116.0	1.89	2.16

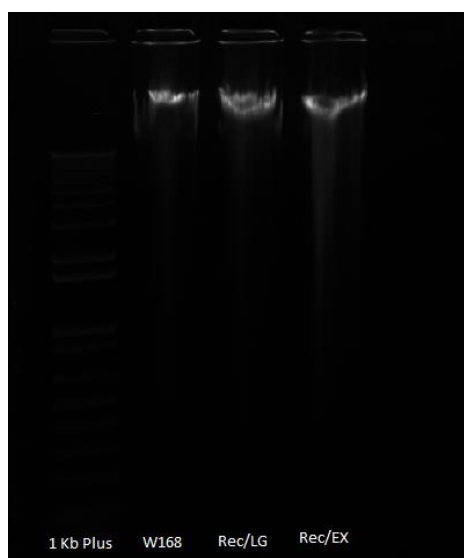


Figure 10: 1% agarose gel of genomic DNA extracted from the parents of W168, Rec/LG, and Rec/EX using the optimised method.

Unfortunately, these results could not be reproduced with any of the evolved samples, nor could it be replicated with the parent samples. These samples were also themselves discarded because at the time it was believed they were of insufficient quality for whole genome sequencing.

### 3.3.2 PCR Amplification of the *LeuB* Gene

The Pfx-culture PCR method was able to successfully amplify the *LeuB* gene from 5 of the 30 samples. These were the W168 and Rec/LG parents, as well as Gen54 W168 A, Rec/LG B, and Rec/LG C. The Pfx-glycerol method was used to successfully amplify 4 samples, these being the Rec/EX parent, as well as Gen54 W168 B, W168 C, and Rec/LG A. The HF-glycerol method successfully amplified 5 samples, these being the Gen199 W168 A, W168 B, W168 C, Rec/LG A, and Rec/LG C samples.

Unfortunately, after clean-up of the PCR products, there was insufficient yield for sequencing in all but the parent samples.

### **3.3.3 Heterogeneity of Evolved Samples**

Throughout the PCR amplification experiments, it became apparent that there was a substantial difference between evolved samples. Methods that were successful for some samples would produce insufficient or no results for others. Furthermore, samples from the later generations of the evolution experiment were more difficult to amplify the *LeuB* gene from than those from earlier generations. For example, PCR was never successful on any sample from Gen298, regardless of the method used. This heterogeneity became the basis for a series of morphological experiments. The intention of these experiments was to link difficulties in PCR amplification to phenotypic changes in the evolved samples.

# Morphology of Evolved *Bacillus subtilis*

---

## 4.1 Introduction

Over the course of the genetics experiments, it became clear that there were substantial phenotypic differences between evolved samples. PCR methods that worked well for some samples would barely work, or not work at all, for others. Furthermore, some of the evolved samples of *B. subtilis* took on a very different colony morphology when growing on agar plates. Based on these observations, a series of experiments were devised and carried out to better understand the heterogeneity that had cropped up amongst the evolved samples and compare this with the experienced difficulties in PCR amplification.

## 4.2 Methods

### 4.2.1 Plate Growth

All plates used in the morphology experiments were LB agar, made up in water with 1% w/v Bacto Peptone, 0.5% w/v yeast extract, 1% w/v NaCl, and 1.5% w/v Bacto Agar. Glycerol stocks of evolved samples were streaked out onto plates and incubated at 37 °C overnight. Some agar plates were instead left to grow for 48 hrs in order to observe colony growth over a longer time period.

### 4.2.2 Endospore Staining

Cultures were smeared onto microscope slides using water, then dried and fixed with a Bunsen burner. Small sections of tissue paper were used to cover the smears, to aid retention of the malachite green stain and prevent spillage. Smears were flooded with a 5% w/v aqueous solution of malachite green and heated with a Bunsen burner to the point of light steaming for 60 seconds. Extra malachite green solution was added as necessary to stop the smear from drying out. Excess malachite green was then washed off, and the smear was counterstained with a 0.5% w/v aqueous solution of safranin for 30 seconds. The safranin was washed off and the smears were allowed to air dry.

## 4.3 Results

### 4.3.1 Colony Morphology

The evolved samples can be clearly split into two groups based on colony morphology when grown on agar plates. Some displayed the wildtype morphotype of large colonies with fimbriated edges, which comfortably fits descriptions of *B. subtilis* colony growth in the literature. Maughan & Nicholson in 2011 define this as the large colony morphotype (LCM), which is the term that will be used in this thesis for the wildtype henceforth. Others developed a new colony morphotype (NCM). Figures 11-13 show the progressive adoption of this new morphotype over the generations of the evolution experiment.

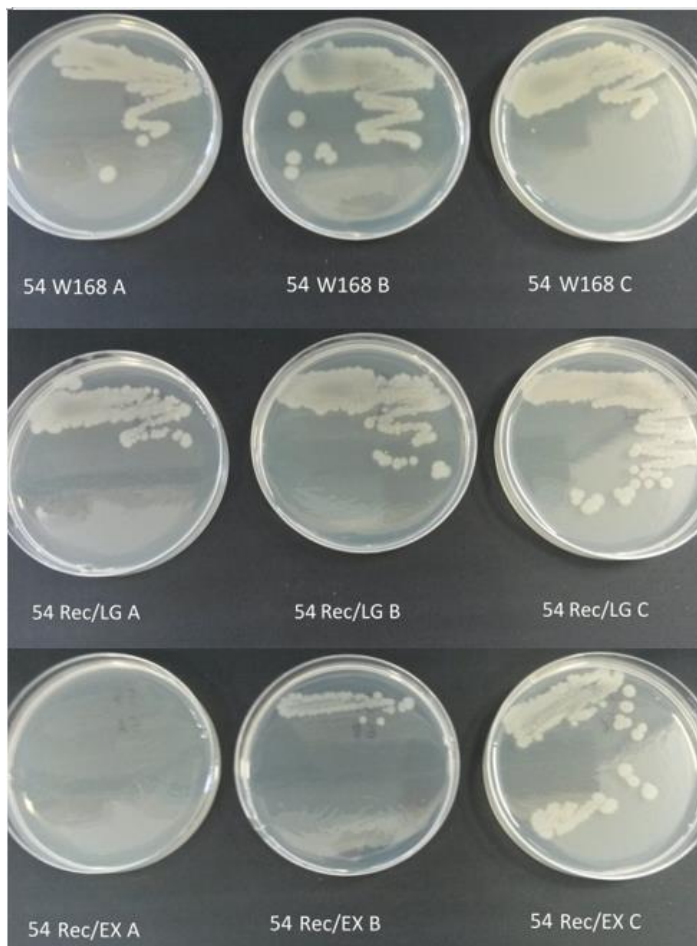


Figure 11: Evolved samples from generation 54 grown on agar plates, illustrating differences in colony morphotype.

The NCM had already begun to appear by generation 54, the earliest generation for which glycerol stocks exist. At this point, it is affecting only a single strain, Rec/EX

A. The NCM is defined by its poor growth on the LB agar. After 24 hrs, it appears as an amorphous smear around the areas where the glycerol stock was initially streaked, in contrast to the distinct, feathered colonies of the LCV. Some distinct colonies can form at this point for NCM samples, but they are small enough to be missed if not looking closely and do not always appear.

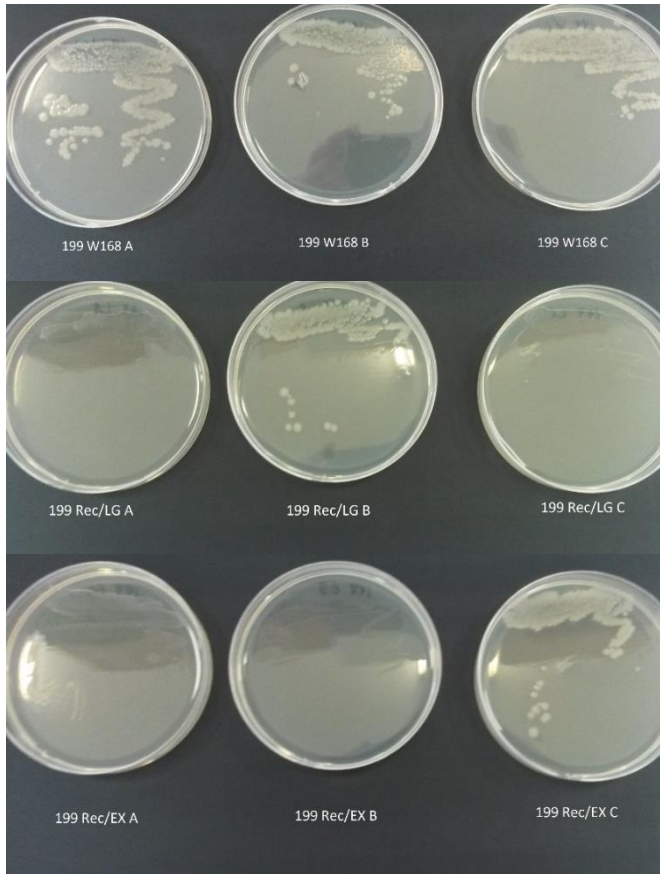


Figure 12: Evolved samples from generation 199 grown on agar plates, illustrating differences in colony morphotype.

By generation 199, the NCM had appeared in 4 of the 9 strains.



Figure 13: Evolved samples from generation 298 grown on agar plates, all displaying the NCM.

By generation 298, all strains had adopted the NCM.

### 4.3.2 Growth of the New Morphotype

Samples possessing the NCM grew poorly on LB agar plates compared to those with the wild type morphotype. Figure 14 shows the growth of generation 298 W168 samples, which possess the NCM, after 24 hrs. The bacteria are visible as a faint, amorphous smear. Distinct colonies can be very faintly seen in 298 W168 C.

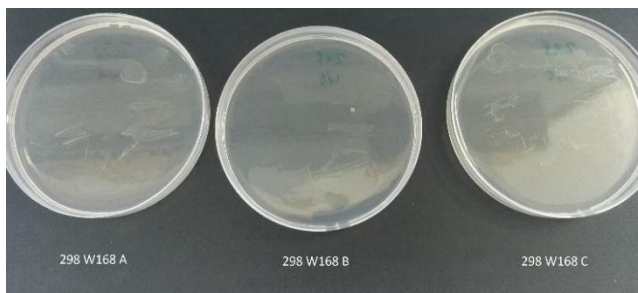


Figure 14: W168 samples from generation 298 after 24 hrs of growth on agar plates.

Figure 15 shows the growth of the generation 298 W168 samples after 48 hrs. The bacteria become much more visible, and distinct colonies become far more apparent. These colonies are far smaller than those formed by the samples with the LCM. The edges of these colonies are also regular, in contrast to the feathery, fimbriated edges of the LCM .



Figure 15: W168 samples from generation 298 after 48 hrs of growth on agar plates.

### 4.3.3 Sporulation and Cell Morphology

After growing overnight on LB agar, all samples which possessed the LCM had begun sporulation. Those samples which had adopted the NCM either did not sporulate or had far fewer spores under the same conditions. Figures 16-18 show the degree of sporulation in the different samples. Spores, where present, are visible as green spheres or short rods.

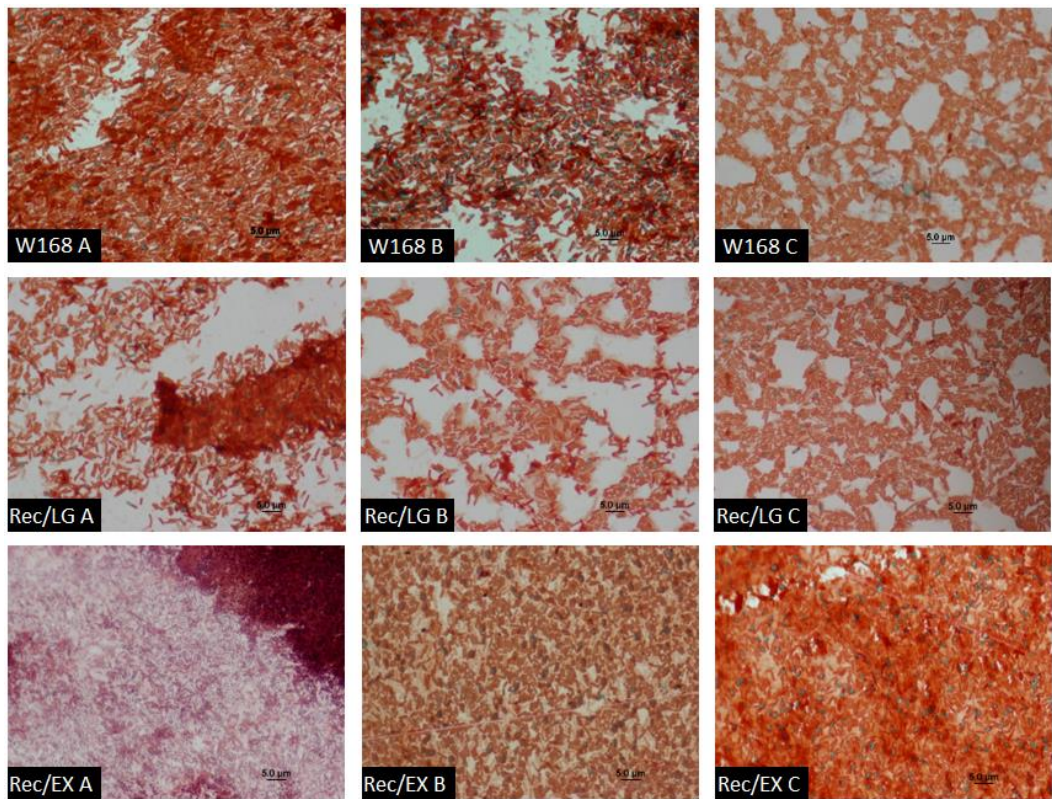


Figure 16: Cells from generation 54 after endospore staining.

A moderate amount of sporulation is common in samples from generation 54. The exception to this is Rec/EX A, which appears to have no spores whatsoever. Of the generation 54 samples, Rec/EX A is the only one with the NCM. Rec/EX A also has a far more purple tint than the other samples, and the individual cells are smaller.

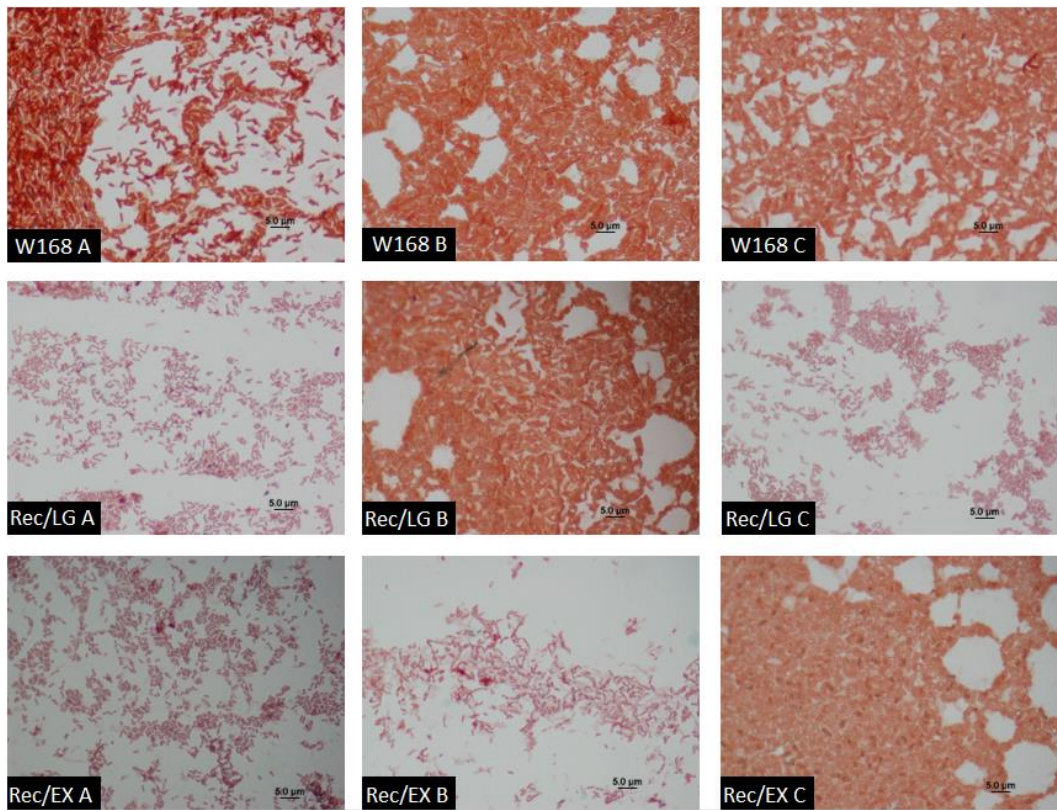


Figure 17: Cells from generation 199 after endospore staining.

By generation 199, sporulation has become less common. Only W168 A, W168 C, and Rec/EX C unambiguously show spores or spore formation. Rec/LG A, Rec/LG C, and Rec/EX B have all adopted the purple colouration and smaller cell size that was already exhibited by Rec/EX A in generation 54. This cellular phenotype continues to correlate exactly with the NCM.

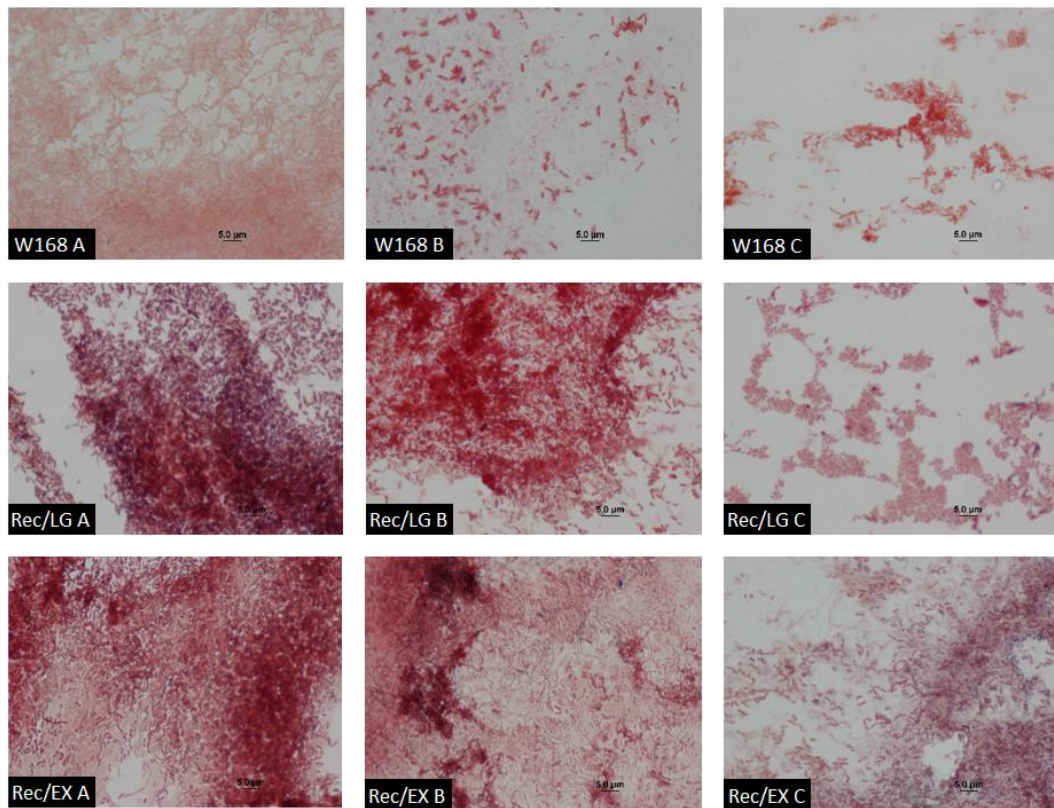


Figure 18: Cells from generation 298 after endospore staining.

Only Rec/EX B and Rec/EX C unambiguously show spores among the generation 298 samples. W168 B, Rec/LG A, Rec/LG B, Rec/LG C, and Rec/EX A show dark spots that could be the early stages of sporulation, but this is unclear. By generation 298, all samples have adopted the smaller cell phenotype. Despite all samples displaying the NCM, not all have the same purple tint shown in earlier generations. W168 A, W168 B, W168 C, and Rec/LG B, seem to have retained the red colouration typical of LCM samples.

The NCM first appeared in slightly over 50 generations, and swept to fixation in 9 independent populations within 300 generations. All 9 strains of the NCM share the traits of slow growth on LB agar plates, small colonies lacking a fimbriated edge, and small cells. The colony shape and size of the NCM are similar to the SCV described by Maughan & Nicholson in 2011.

# Discussion and Future Research

---

## 5.1 Structure of Rec/LG and Rec/EX

The crystal structures of neither Rec/LG nor Rec/EX were solved over the duration of this project. However, both proteins were successfully crystallised several times, providing a solid basis for further optimisation. The obvious direction to take this research in the future is to continue trying to obtain crystals of Rec/LG and Rec/EX that are large enough to use in X-Ray diffraction. The crystallisation conditions used to grow the crystals in Figure 4 (see appendix) are good starting points for further optimisation. Techniques such as crystal seeding could be used to try and increase the size of the crystals.

SWISS-Model was used to generate a model of the structures of Rec/LG and Rec/EX. The crystal structure of ANC4 was used as the template for these models due to the high sequence similarity between it, Rec/LG, and Rec/EX. The 3D structure of these models was almost identical to that of ANC4, and the active sites in particular were extremely well conserved as expected from the high level of conservation in this region amongst LeuB enzymes. Indeed, the distantly related *T. thermophilus* shares most of its active site residues with the three resurrected LeuB ancestors. However, the almost identical positioning of the residues may be an artefact of the modelling method.

The models of Rec/LG and Rec/EX did not offer any significant insight into the structural basis of the kinetic differences between Rec/LG, Rec/EX, and ANC4. The most evident disconnect between structure and kinetics is the high  $K_M^{(NAD)}$  for Rec/EX, and to a lesser extent Rec/LG. The NAD binding sites of these enzymes is only different from ANC4 by a single amino acid – isoleucine in Rec/LG and Rec/EX instead of leucine in ANC1. While possible, it seems unlikely that this miniscule change could explain the almost four-fold increase in  $K_M^{(NAD)}$  between ANC4 and Rec/LG, nor the more than six-fold increase between ANC4 and Rec/EX. LeuB does take on significantly different conformations when binding both NAD (Kadono *et al.* 1995) and IPM (Imada *et al.* 1998). The crystal structure for ANC4,

and so the models of Rec/LG and Rec/EX, are in the open conformation typical of LeuB not bound to any ligands. It is possible that the structural features behind the large difference between  $K_M^{(NAD)}$  in these enzymes are only present in different conformations. But again, it is possible that the modelling method used simply overestimated the similarity between Rec/LG, Rec/EX, and ANC1.

Without the experimentally determined crystal structures of Rec/LG and Rec/EX, it is impossible to know exactly how accurate the model structures are. However, the QMEAN and GMQE scores assigned to the models suggest that they are reliable. Any further research into the structural basis of the kinetic properties of Rec/LG and Rec/EX will require a structure generated from empirical data rather than a statistical model.

## **5.2 Genetics of Evolved Samples**

### **5.2.1 Whole Genome DNA Extraction**

Whole genome sequencing of the 3 parent and 27 evolved samples is essential for uncovering the genetic changes that occurred during the course of the experiment and to suggest reasons for their new phenotypes. Next generation sequencing techniques used in modern genome sequencing are dependent on having a good amount of high quality DNA to work with (Doyle 2015). The requirement of extracting DNA with high yields, low contamination, and minimal DNA degradation from the 30 samples of this project proved a significant challenge. Methods that produced clean, intact DNA had low yields. Methods that produced sufficient yields suffered either from high contamination, highly degraded DNA, or both.

Although the optimised method of genomic DNA extraction outlined in Chapter 3 was able to produce DNA of sufficient yield and quality for whole genome sequencing, it could not be replicated. The addition of RNase A to a completed DNA extraction resulted in extremely clean bands of high molecular weight genomic DNA with high yield. It suffered heavily from contamination of both phenol and protein, but these may not be difficult issues to remedy. A DNA

extraction method which used chloroform instead of phenol chloroform would remove the issue of phenol contamination, and a wide variety of methods and kits are capable of removing proteins from a solution.

Brown *et al.* in 2011 extracted DNA from one of the SCV strains of the 6,000 generation *B. subtilis* evolution experiment for use in whole genome sequencing. Since the evolved samples of this project were grown in a similar spore repressing medium and appear to be somewhat similar to the SCV strains, the methods used by Brown *et al.* could work for the evolved samples of this project.

### **5.2.2 PCR Amplification of *leuB***

PCR amplification of the *leuB* gene was attempted once it became apparent that extraction of high quality whole genome DNA might not happen within the timeframe of this project. The hope for the evolution experiment was, and still is, that the ancestral *leuB* genes of the Rec/LG and Rec/EX strains would mutate in some significant way over the course of the experiment towards the contemporary version. PCR was considered as a way to quickly get a snapshot of the *leuB* gene to see if any such mutation had occurred in any of the 9 strains. Unfortunately, the PCR experiments ran into problems of their own. Initial attempts at PCR were unsuccessful due to faulty primers. Once the fault with these primers was fixed, they would work on control samples but bizarrely not with any of the parent or evolved samples of the evolution experiment. Between these two issues, a lot of time was lost before any PCR products were successfully generated.

The first successes with amplifying *leuB* came from using a second set of primers that sat closer to the start and end of the gene, which had been successful during Dr. Andrews' initial pilot attempts at amplifying *leuB*. These primers were avoided at first for this project due to concerns that the start and end of the gene sequences would be unreliable, and so valuable information could be lost. Even with the alternative primers, amplifying *leuB* from the 30 samples was an unreliable process. Many more small variations or different methods were tried than the at least partially successful ones outlined in this thesis. Any given method would either not work at all, or work for a seemingly random selection of samples. The only clear

indication of a trend amongst which samples were working and which ones weren't came with the HF-glycerol method. Used on all samples of generation 199, it only worked on the 5 that were later classified to have the LCM. The 4 samples with the NCM didn't amplify at all. Furthermore, the HF-glycerol method didn't work for any of the 9 samples of generation 298, all of which have the NCM. It is unknown why NCM strains are difficult to perform PCR on. The NCM shares some similarities with the SCV that developed during the 6,000 generation evolution experiment, but none of the studies dealing with the SCV strains have expressed difficulties in working with them. It is possible that any such difficulties were simply not reported, or that the apparent resistance to PCR is unique to the NCM.

Future efforts to uncover the genetics of this evolution experiment should focus of whole genome sequencing, which will provide far more information.

### **5.3 Morphology of Evolved *Bacillus subtilis***

#### **5.3.1 Phenotypic Differences Between Samples**

The poor growth of evolved samples of *B. subtilis* on agar plates was first recorded by Dr. Andrews at the conclusion of the evolution experiment. Due to the focus of the experiment at this time on the genetics of the samples, rather than their phenotype, this poor growth was noted but not fully characterised. It was not until the failure of the HF-glycerol PCR method correlated with this poor growth that efforts were made to characterise the physical changes that the evolved samples had undergone.

The NCM was initially characterised as an amorphous smear with poor growth, in contrast to the large and distinct colonies formed by samples with the LCM. LB agar is a nutrient rich medium, and should be an ideal environment for *B. subtilis* to grow on. The poor growth of the NCM samples on this medium indicates that they have evolved to become niche specialists which have adapted for rapid growth in the spore repressing medium used for the evolution experiment. Despite the initial observations that NCM samples did not form distinct colonies on agar plates, it became clear that they do when given enough time to grow. The colonies formed

by the NCM samples were much smaller than those formed by samples with the LCM.

It was not only the colony morphology of the samples that changed during the evolution experiment. The endospore staining experiment revealed several differences in cell morphology that correlate exactly with presence of the NCM. The first is greatly reduced or lack of sporulation after growing on agar plates for 24 hrs. This is likely due to the poor growth of NCM samples on agar plates preventing them from reaching a nutrient limiting point after 24 hrs, rather than any actual change in the cells' ability to sporulate. Supporting this is the evidence of slight sporulation in some of the NCM samples. Cells of the NCM samples are also noticeably smaller than their LCM counterparts. Though not common to all strains, some NCM samples have taken on a rather more purple colouration in response to the endospore staining process. This purple colouration might imply changes to the cell membrane which caused the counterstain safranin to bind differently. Such changes to the membrane could also help to explain the difficulties with performing PCR on the evolved samples, although this is complete speculation.

### **5.3.2 Comparing NCM to SCV**

In 2011, Maughan & Nicholson reported on one of the many findings from their 6,000 generation *B. subtilis* evolution experiment. This paper detailed the emergence of a new colony morphotype in several strains which they called the Small Colony Variant (SCV). The SCV became fixed in four out of five strains that were grown in sporulation repressing medium. When allowed to grow for 48 hrs and reach a point where distinct colonies start forming, NCM samples look similar to Maughan & Nicholson's SCV.

Interestingly, the SCV took much longer to appear than the NCM. The earliest onset of the SCV occurred around generation 1,330, while the latest it appeared was in generation 4,214 (appearing for a second time after being lost earlier in that strain's evolution). In one of the five spore repressing strains, the SCV never appeared. This is in stark contrast to the development of the NCM. First appearing by generation 54, and possibly even earlier, it swept to fixation by generation 298 for all 9 strains.

The NCM evolved much faster in this experiment than the SCV did in the 6,000 generation evolution experiment. It is possible that this is due to differences in the evolution media used. While the 6,000 generation experiment used a complete media, the media used for this experiment lacked almost all amino acids. The need to synthesize amino acids may have placed a greater selective pressure on the evolving strains, leading to the much faster adoption of a new phenotype.

Despite their similar colony morphologies, NCM and SCV are not identical. Maughan & Nicholson reported that two of their four SCV strains had adopted a long, filamentous cell morphology compared to the usual rod shape of *B. subtilis*. Not only do none of the NCM samples show this filamentous phenotype, but none of the SCV samples show the small cell phenotype that is present in all the NCM samples (Maughan & Nicholson 2011). It is unsurprising that the strains of this experiment did not adopt the same phenotypes as those of the 6,000 generation experiment. After all, evolution is fundamentally random, and unless a phenotype is very advantageous to survival in the type of media used for the evolution experiments, there is no reason to think it would be independently adopted by many different strains. However, considering this it is interesting to note that the samples of this experiment took on a very similar colony morphology to the SCV. This supports the hypothesis of Maughan & Nicholson that the small colony phenotype, or a correlated phenotype, offers a higher fitness in spore repressing media.

Brown *et al.* in 2011 analysed the genomes of different SCV strains. Genomic erosion was common, including degradation of genes involved in sporulation, antibiotic resistance, DNA repair, and some biosynthetic pathways. None of the observed genetic mutations could be tied to the small colony phenotype.

It is also interesting that 9 independent strains all adopted the same colony and cell phenotypes over such a short period of evolutionary time. It took less than 300 generations for the NCM to completely replace the LCM in all 9 strains: This is an incredibly fast and consistent evolutionary change, likely driven by strong selection pressures for amino acid synthesis. The SCV not only took much longer, but it was also much less consistent. Only 4 of the 5 strains adopted it, and among those 4 there was significant variation in cell morphology. The colonies and cells of all 9

strains in our experiment are almost identical, with the only noticeable difference being the degree of purple colouration when subjected to endospore staining with malachite green and safranin.

## **5.4 Conclusions**

Despite several avenues of this project being unsuccessful, some progress has been made. Rec/LG and Rec/EX were both successfully crystallised, and the phenotypes of the evolved samples have been partially characterised. The most significant finding of this project is the extremely rapid emergence of the NCM in all 9 strains, and the similarity of the small colony morphology to the SCV described by Maughan & Nicholson in 2011. Future research should focus on solving the crystal structures of Rec/LG and Rec/EX, fully characterising the NCM phenotype, and sequencing the genomes of all evolved and parent samples in order to better understand what has happened on both the genetic and phenotypic levels.

## References

---

- Akanuma, S., Nakajima, Y., Yokobori, S., Kimura, M., Nemoto, N., Mase, T., . . . Yamagishi, A. (2013). Experimental evidence for the thermophilicity of ancestral life. *Proc Natl Acad Sci U S A*, *110*(27), 11067-11072. doi:10.1073/pnas.1308215110
- Akanuma, S., Yokobori, S., Nakajima, Y., Bessho, M., & Yamagishi, A. (2015). Robustness of predictions of extremely thermally stable proteins in ancient organisms. *Evolution*, *69*(11), 2954-2962. doi:10.1111/evo.12779
- Albery, W. J. K., J. R. (1976). Evolution of Enzyme Function and the Development of Catalytic Efficiency. *Biochemistry*, *15*(25), 5631 - 5640.
- Arnold, K., Bordoli, L., Kopp, J., & Schwede, T. (2006). The SWISS-MODEL workspace: a web-based environment for protein structure homology modelling. *Bioinformatics*, *22*(2), 195-201. doi:10.1093/bioinformatics/bti770
- Bar-Even, A., Noor, E., Savir, Y., Liebermeister, W., Davidi, D., Tawfik, D. S., & Milo, R. (2011). The moderately efficient enzyme: evolutionary and physicochemical trends shaping enzyme parameters. *Biochemistry*, *50*(21), 4402-4410. doi:10.1021/bi2002289
- Beffa, T. B., M.; Lyon, P.; Vogt, G; Marchiani, M.; Fischer, J. L.; Aragno, M. (1996). Isolation of Thermus Strains from Hot Composts (60 to 80°C). *APPLIED AND ENVIRONMENTAL MICROBIOLOGY*, *62*(5), 1723–1727.
- Biasini, M., Bienert, S., Waterhouse, A., Arnold, K., Studer, G., Schmidt, T., . . . Schwede, T. (2014). SWISS-MODEL: modelling protein tertiary and quaternary structure using evolutionary information. *Nucleic Acids Res*, *42*(Web Server issue), W252-258. doi:10.1093/nar/gku340
- Björkman, J. N., I.; Berg, O. G.; Hughes, D.; Andersson, D. I. (2000). Effects of Environment on  
Compensatory Mutations to Ameliorate Costs of Antibiotic Resistance. *Science*, *287*, 1479-1482.
- Bloom, J. D., Labthavikul, S. T., Otey, C. R., & Arnold, F. H. (2006). Protein stability promotes evolvability. *Proceedings of the National Academy of Sciences*, *103*(15), 5869-5874.
- Bridgham, J. T., Ortlund, E. A., & Thornton, J. W. (2009). An epistatic ratchet constrains the direction of glucocorticoid receptor evolution. *Nature*, *461*(7263), 515-519. doi:10.1038/nature08249

- Brown, C. T., Fishwick, L. K., Chokshi, B. M., Cuff, M. A., Jackson, J. M. t., Oglesby, T., . . . Nicholson, W. L. (2011). Whole-genome sequencing and phenotypic analysis of *Bacillus subtilis* mutants following evolution under conditions of relaxed selection for sporulation. *Appl Environ Microbiol*, 77(19), 6867-6877. doi:10.1128/AEM.05272-11
- Burns, R. O. C., J.; Margolin, P.; Umbarger, H. E. (1966). Expression of the Leucine Operon. *Journal of Bacteriology*, 91(4), 1570-1576.
- Burns, R. O. U., H. E.; Gross, S. R. (1963). The Biosynthesis of Leucine. III. The Conversion of  $\alpha$ -Hydroxy-dCarboxyisocaproate to  $\alpha$ -Ketoisocaproate. *Biochemistry*, 2(5), 1053-1058.
- Butzin, N. C., Lapierre, P., Green, A. G., Swithers, K. S., Gogarten, J. P., & Noll, K. M. (2013). Reconstructed ancestral myo-inositol-3-phosphate synthases indicate that ancestors of the Thermococcales and Thermotoga species were more thermophilic than their descendants. *PloS one*, 8(12). doi:10.1371/
- Cai, W., Pei, J., & Grishin, N. V. (2004). Reconstruction of ancestral protein sequences and its applications. *BMC Evol Biol*, 4, 33. doi:10.1186/1471-2148-4-33
- Chi, E. Y., Krishnan, S., Randolph, T. W., & Carpenter, J. F. (2003). Physical stability of proteins in aqueous solution: mechanism and driving forces in nonnative protein aggregation. *Pharmaceutical research*, 20(9), 1325-1336.
- Chinen, A., Matsumoto, Y., & Kawamura, S. (2005). Reconstitution of ancestral green visual pigments of zebrafish and molecular mechanism of their spectral differentiation. *Mol Biol Evol*, 22(4), 1001-1010. doi:10.1093/molbev/msi086
- Cole, M. F., & Gaucher, E. A. (2011). Utilizing natural diversity to evolve protein function: applications towards thermostability. *Curr Opin Chem Biol*, 15(3), 399-406. doi:10.1016/j.cbpa.2011.03.005
- Dean, A. M. D., L. (1995). The role of glutamate 87 in the kinetic mechanism of *Thermus thermophilus* isopropylmalate dehydrogenase. *Protein Science*, 4, 2156-2167.
- Dellus-Gur, E., Toth-Petroczy, A., Elias, M., & Tawfik, D. S. (2013). What makes a protein fold amenable to functional innovation? Fold polarity and stability trade-offs. *J Mol Biol*, 425(14), 2609-2621. doi:10.1016/j.jmb.2013.03.033
- DePristo, M. A., Weinreich, D. M., & Hartl, D. L. (2005). Missense meanderings in sequence space: a biophysical view of protein evolution. *Nat Rev Genet*, 6(9), 678-687. doi:10.1038/nrg1672

- Doyle, K. (2015). Quantitation in Next-Generation Sequencing Library Workflows.
- Dykhuizen, D. (1990). EXPERIMENTAL STUDIES OF NATURAL SELECTION IN BACTERIA. *Annual Review of Ecology*, 21, 373-398.
- Eick, G. N., Colucci, J. K., Harms, M. J., Ortlund, E. A., & Thornton, J. W. (2012). Evolution of minimal specificity and promiscuity in steroid hormone receptors. *PLoS Genet*, 8(11), e1003072. doi:10.1371/journal.pgen.1003072
- Fields, P. A. (2001). Review: Protein function at thermal extremes: balancing stability and flexibility. *Comparative Biochemistry and Physiology Part A: Molecular & Integrative Physiology*, 192(2), 417-431.
- Garrett, R. H., & Grisham, C. M. (2005). *Biochemistry*, Thomson Learning. Inc., Stamford, Conn.
- Gaucher, E. A., Govindarajan, S., & Ganesh, O. K. (2008). Palaeotemperature trend for Precambrian life inferred from resurrected proteins. *Nature*, 451(7179), 704-707. doi:10.1038/nature06510
- Gaucher, E. A., Thomson, J. M., Burgan, M. F., & Benner, S. A. (2003). Inferring the palaeoenvironment of ancient bacteria on the basis of resurrected proteins. *Nature*, 425(6955), 285-288.
- Giulio, M. D. (2003). The Universal Ancestor was a Thermophile or a Hyperthermophile: Tests and Further Evidence. *Journal of Theoretical Biology*, 221(3), 425-436. doi:10.1006/jtbi.2003.3197
- Graczer, E., Merli, A., Singh, R. K., Karuppasamy, M., Zavodszky, P., Weiss, M. S., & Vas, M. (2011). Atomic level description of the domain closure in a dimeric enzyme: thermus thermophilus 3-isopropylmalate dehydrogenase. *Mol Biosyst*, 7(5), 1646-1659. doi:10.1039/c0mb00346h
- Granhölm, K., Leo Harju, and Ari Ivaska. (2009). Desorption of metal ions from kraft pulps. Part 1. Chelation of hardwood and softwood kraft pulp with EDTA. *BioResources*, 5(1), 206-226.
- Greco, M., Chiappetta, A., Bruno, L., & Bitonti, M. B. (2012). In *Posidonia oceanica* cadmium induces changes in DNA methylation and chromatin patterning. *J Exp Bot*, 63(2), 695-709. doi:10.1093/jxb/err313
- Groussin, M., Hobbs, J. K., Szollosi, G. J., Gribaldo, S., Arcus, V. L., & Gouy, M. (2015). Toward more accurate ancestral protein genotype-phenotype reconstructions with the use of species tree-aware gene trees. *Mol Biol Evol*, 32(1), 13-22. doi:10.1093/molbev/msu305
- Guex, N., Peitsch, M. C., & Schwede, T. (2009). Automated comparative protein structure modeling with SWISS-MODEL and Swiss-PdbViewer: a

historical perspective. *Electrophoresis*, 30 Suppl 1, S162-173.  
doi:10.1002/elps.200900140

Hall, B. G. (2006). Simple and accurate estimation of ancestral protein sequences. *Proceedings of the National Academy of Sciences*, 103(14), 5431-5436.

Hanson-Smith, V., Kolaczkowski, B., & Thornton, J. W. (2010). Robustness of ancestral sequence reconstruction to phylogenetic uncertainty. *Mol Biol Evol*, 27(9), 1988-1999. doi:10.1093/molbev/msq081

Harms, M. J., & Thornton, J. W. (2010). Analyzing protein structure and function using ancestral gene reconstruction. *Curr Opin Struct Biol*, 20(3), 360-366. doi:10.1016/j.sbi.2010.03.005

Hobbs, J. K., Prentice, E. J., Groussin, M., & Arcus, V. L. (2015). Reconstructed Ancestral Enzymes Impose a Fitness Cost upon Modern Bacteria Despite Exhibiting Favourable Biochemical Properties. *J Mol Evol*, 81(3-4), 110-120. doi:10.1007/s00239-015-9697-5

Hobbs, J. K., Shepherd, C., Saul, D. J., Demetras, N. J., Haaning, S., Monk, C. R., . . . Arcus, V. L. (2011). On the origin and evolution of thermophily: reconstruction of functional precambrian enzymes from ancestors of *Bacillus*. *Mol Biol Evol*, 29(2), 825-835. doi:10.1093/molbev/msr253

Imada, K., Sato, M., Tanaka, N., Katsube, Y., Matsuura, Y., & Oshima, T. (1991). Three-dimensional structure of a highly thermostable enzyme, 3-isopropylmalate dehydrogenase of *Thermus thermophilus* at 2.2 Å resolution. *Journal of Molecular Biology*, 222(3), 725-738.  
doi:[https://doi.org/10.1016/0022-2836\(91\)90508-4](https://doi.org/10.1016/0022-2836(91)90508-4)

Imada, K. I., K.; Matsunami, H.; Kawaguchi, H.; Tanaka, H.; Tanaka, N.; Namba, K. (1998). Structure of 3-isopropylmalate dehydrogenase in complex with 3-isopropylmalate at 2.0 Å resolution: the role of Glu88 in the unique substrate-recognition mechanism. *Structure*, 6, 971-982.

Joy, J. B., Liang, R. H., McCloskey, R. M., Nguyen, T., & Poon, A. F. (2016). Ancestral Reconstruction. *PLoS Comput Biol*, 12(7), e1004763.  
doi:10.1371/journal.pcbi.1004763

Kadono, S. S., M.; Moriyama, H.; Sato, M.; Hayashi, Y.; Oshima, T.; Tanaka, N. (1995). Ligand-Induced Changes in the Conformation of 3-Isopropylmalate Dehydrogenase from *Thermus thermophilus*. *Biochemistry*, 118(4), 745-752.

Kagawa, Y. N., H.; Nukiwa, N.; Ishizuka, M.; Nakajima, T.; Yasuhara, T.; Tanaka, T.; Oshima, T. (1984). High Guanine plus Cytosine Content in the Third Letter of Codons of an Extreme Thermophile. *The Journal of Biological Chemistry*, 259(5), 2956-2960.

Kenniston, J. A., Baker, T. A., Fernandez, J. M., & Sauer, R. T. (2003). Linkage between ATP Consumption and Mechanical Unfolding during the Protein

Processing Reactions of an AAA+ Degradation Machine. *Cell*, 114(4), 511-520. doi:10.1016/s0092-8674(03)00612-3

Khersonsky, O., & Tawfik, D. S. (2010). Enzyme promiscuity: a mechanistic and evolutionary perspective. *Annu Rev Biochem*, 79, 471-505. doi:10.1146/annurev-biochem-030409-143718

Kiefer, F., Arnold, K., Kunzli, M., Bordoli, L., & Schwede, T. (2009). The SWISS-MODEL Repository and associated resources. *Nucleic Acids Res*, 37(Database issue), D387-392. doi:10.1093/nar/gkn750

Kirino, H., Aoki, M., Aoshima, M., Hayashi, Y., Ohba, M., Yamagashi, A., ... & Oshima, T. (1994). Hydrophobic interaction at the subunit interface contributes to the thermostability of 3-isopropylmalate dehydrogenase from an extreme thermophile, *Thermus thermophilus*. *The FEBS Journal*, 220(1), 275-281.

Krishnan, N. M., Seligmann, H., Stewart, C. B., De Koning, A. P., & Pollock, D. D. (2004). Ancestral sequence reconstruction in primate mitochondrial DNA: compositional bias and effect on functional inference. *Mol Biol Evol*, 21(10), 1871-1883. doi:10.1093/molbev/msh198

Lazar, V., Pal Singh, G., Spohn, R., Nagy, I., Horvath, B., Hrtyan, M., . . . Pal, C. (2013). Bacterial evolution of antibiotic hypersensitivity. *Mol Syst Biol*, 9, 700. doi:10.1038/msb.2013.57

Lenski, R. E. (1998). Bacterial evolution and the cost of antibiotic resistance. *International Microbiology*, 1, 265-270.

Loughran, N. B., O'Connell, M. J., O'Connor, B., & O'Fagain, C. (2014). Stability properties of an ancient plant peroxidase. *Biochimie*, 104, 156-159. doi:10.1016/j.biochi.2014.05.012

Lunzer, M., Golding, G. B., & Dean, A. M. (2010). Pervasive cryptic epistasis in molecular evolution. *PLoS Genet*, 6(10). doi:10.1371/

10.1371/journal.pgen.1001162.g001

Mader, U., Schmeisky, A. G., Florez, L. A., & Stulke, J. (2012). SubtiWiki--a comprehensive community resource for the model organism *Bacillus subtilis*. *Nucleic Acids Res*, 40(Database issue), D1278-1287. doi:10.1093/nar/gkr923

Malcolm, B. A., Wilson, K. P., Matthews, B. W., Kirsch, J. F., & Wilson, A. C. (1990). Ancestral lysozymes reconstructed, neutrality tested, and thermostability linked to hydrocarbon packing. *Nature*, 345(6270), 86.

Maughan, H., Masel, J., Birky, C. W., Jr., & Nicholson, W. L. (2007). The roles of mutation accumulation and selection in loss of sporulation in experimental populations of *Bacillus subtilis*. *Genetics*, 177(2), 937-948. doi:10.1534/genetics.107.075663

- Maughan, H., & Nicholson, W. L. (2011). Increased fitness and alteration of metabolic pathways during *Bacillus subtilis* evolution in the laboratory. *Appl Environ Microbiol*, *77*(12), 4105-4118. doi:10.1128/AEM.00374-11
- Maughan, H. C., V.; Hancock, A.; Birky, C. W.; Nicholson, W. L.; Masel, J. (2006). The Population Genetics of Phenotypic Deterioration in Experimental Populations of *Bacillus subtilis*. *Evolution*, *60*(4), 686-695.
- Merkl, R., & Sterner, R. (2016). Ancestral protein reconstruction: techniques and applications. *Biol Chem*, *397*(1), 1-21. doi:10.1515/hsz-2015-0158
- Newton, M. S., Arcus, V. L., & Patrick, W. M. (2015). Rapid bursts and slow declines: on the possible evolutionary trajectories of enzymes. *J R Soc Interface*, *12*(107). doi:10.1098/rsif.2015.0036
- O'Malley, M. A. (2017). The Experimental Study of Bacterial Evolution and Its Implications for the Modern Synthesis of Evolutionary Biology. *J Hist Biol*. doi:10.1007/s10739-017-9493-8
- Ortlund, E. A., Bridgham, J. T., Redinbo, M. R., & Thornton, J. W. (2007). Crystal structure of an ancient protein: evolution by conformational epistasis. *Science*, *317*(5844), 1544-1548. doi:10.1126/science.1142819
- Papadopoulos, D. S., D.; Meier-Eiss, J.; Arber, W.; Lenski, R. E.; Blot, M. (1999). Genomic evolution during a 10,000-generation experiment with bacteria. *Proceedings of the National Academy of Sciences of the United States of America*, *96*, 3807-3812.
- Paterson, S., Vogwill, T., Buckling, A., Benmayor, R., Spiers, A. J., Thomson, N. R., . . . Brockhurst, M. A. (2010). Antagonistic coevolution accelerates molecular evolution. *Nature*, *464*(7286), 275-278. doi:10.1038/nature08798
- Perez-Jimenez, R., Inglés-Prieto, A., Zhao, Z. M., Sanchez-Romero, I., Alegre-Cebollada, J., Kosuri, P., ... & Sanchez-Ruiz, J. M. (2011). Single-molecule paleoenzymology probes the chemistry of resurrected enzymes. *Nature Structural and Molecular Biology*, *18*(5), 592.
- Phillips, P. C. (2008). Epistasis--the essential role of gene interactions in the structure and evolution of genetic systems. *Nat Rev Genet*, *9*(11), 855-867. doi:10.1038/nrg2452
- Prentice, E. J. (2013). Characterisation of Enzyme Evolution through Ancestral Enzyme Reconstruction.
- Risso, V. A., Gavira, J. A., Mejia-Carmona, D. F., Gaucher, E. A., & Sanchez-Ruiz, J. M. (2013). Hyperstability and substrate promiscuity in laboratory resurrections of Precambrian beta-lactamases. *J Am Chem Soc*, *135*(8), 2899-2902. doi:10.1021/ja311630a

- Shoichet, B. K., Baase, W. A., Kuroki, R., & Matthews, B. W. (1995). A relationship between protein stability and protein function. *Proceedings of the National Academy of Sciences*, 92(2), 452-456.
- Somero, G. N. (1995). Proteins and temperature. *Annual review of physiology*, 57.
- Svingor, A., Kardos, J., Hajdu, I., Nemeth, A., & Zavodszky, P. (2001). A better enzyme to cope with cold. Comparative flexibility studies on psychrotrophic, mesophilic, and thermophilic IPMDHs. *J Biol Chem*, 276(30), 28121-28125. doi:10.1074/jbc.M104432200
- Szollosi, G. J., Tannier, E., Daubin, V., & Boussau, B. (2015). The inference of gene trees with species trees. *Syst Biol*, 64(1), e42-62. doi:10.1093/sysbio/syu048
- Tokuriki, N., Stricher, F., Serrano, L., & Tawfik, D. S. (2008). How protein stability and new functions trade off. *PLoS Comput Biol*, 4(2). doi:10.1371/
- Tokuriki, N., & Tawfik, D. S. (2009). Stability effects of mutations and protein evolvability. *Curr Opin Struct Biol*, 19(5), 596-604. doi:10.1016/j.sbi.2009.08.003
- Voordeckers, K., Brown, C. A., Vanneste, K., van der Zande, E., Voet, A., Maere, S., & Verstrepen, K. J. (2012). Reconstruction of ancestral metabolic enzymes reveals molecular mechanisms underlying evolutionary innovation through gene duplication. *PLoS Biol*, 10(12), e1001446. doi:10.1371/journal.pbio.1001446
- Wallon, G., Yamamoto, K., Kirino, H., Yamagishi, A., Lovett, S. T., Petsko G. A., Oshima T. (1996). Purification, catalytic properties and thermostability of 3-isopropylmalate dehydrogenase from *Escherichia coli*. *Biochimica et Biophysica Acta (BBA) - Protein Structure and Molecular Enzymology*, 1337(1), 105-112.
- Wallon, G. K., G.; Lovett, S. T.; Oshima, T.; Ringe, D.; Petsko, G. A. (1997). Crystal Structures of *Escherichia coli* and *Salmonella typhimurium* 3-Isopropylmalate Dehydrogenase and Comparison with their Thermophilic Counterpart from *Thermus thermophilus*. *Journal of Molecular Biology*, 266, 1016-1031.
- Wheeler, L. C., Lim, S. A., Marqusee, S., & Harms, M. J. (2016). The thermostability and specificity of ancient proteins. *Curr Opin Struct Biol*, 38, 37-43. doi:10.1016/j.sbi.2016.05.015
- Whitfield, J. H., Zhang, W. H., Herde, M. K., Clifton, B. E., Radziejewski, J., Janovjak, H., . . . Jackson, C. J. (2015). Construction of a robust and sensitive arginine biosensor through ancestral protein reconstruction. *Protein Sci*, 24(9), 1412-1422. doi:10.1002/pro.2721

- Wiebe, W. J., Sheldon, JR., and Pomeroy, L. R. (1992). Bacterial Growth in the Cold: Evidence for an Enhanced Substrate Requirement. *APPLIED AND ENVIRONMENTAL MICROBIOLOGY*, 58(1), 359-364.
- Williams, P. D., Pollock, D. D., Blackburne, B. P., & Goldstein, R. A. (2006). Assessing the accuracy of ancestral protein reconstruction methods. *PLoS Comput Biol*, 2(6), e69. doi:10.1371/journal.pcbi.0020069
- Woods, R. S., D.; Winkworth, C. L.; Riley, M. A.; Lenski, R. E. (2006). Tests of parallel molecular evolution in a long-term experiment with *Escherichia coli*. *Proceedings of the National Academy of Sciences of the United States of America*, 103(24), 9107-9112.
- Yokoyama, S., Yang, H., & Starmer, W. T. (2008). Molecular basis of spectral tuning in the red- and green-sensitive (M/LWS) pigments in vertebrates. *Genetics*, 179(4), 2037-2043. doi:10.1534/genetics.108.090449
- Zhang, J., & Nei, M. (1997). Accuracies of ancestral amino acid sequences inferred by the parsimony, likelihood, and distance methods. *Journal of molecular evolution*, 44(1), S139-S146.

# Appendix

---

## **Evolution Medium**

100 mM  $\text{KH}_2\text{PO}_4$

3 mM Sodium Citrate

0.3 mM  $\text{MgSO}_4$

0.125% Glucose

0.1% Monopotassium L-Glutamate

2.2 g/L Ammonium Iron III Citrate (Ferric)

5 g/L Tryptophan

## Fine Screens

The following is a complete record of all crystallisation conditions used in fine screens for both Rec/LG and Rec/EX.

Rec/LG (9 mg/mL): Citric acid pH 3.5 + PEG 200

0.05 M Citric acid pH 3.5 26 % Polyethylene glycol 200	0.05 M Citric acid pH 3.5 30 % Polyethylene glycol 200	0.05 M Citric acid pH 3.5 34 % Polyethylene glycol 200	0.05 M Citric acid pH 3.5 38 % Polyethylene glycol 200	0.05 M Citric acid pH 3.5 42 % Polyethylene glycol 200	0.05 M Citric acid pH 3.5 46 % Polyethylene glycol 200
0.10 M Citric acid pH 3.5 26 % Polyethylene glycol 200	0.10 M Citric acid pH 3.5 30 % Polyethylene glycol 200	0.10 M Citric acid pH 3.5 34 % Polyethylene glycol 200	0.10 M Citric acid pH 3.5 38 % Polyethylene glycol 200	0.10 M Citric acid pH 3.5 42 % Polyethylene glycol 200	0.10 M Citric acid pH 3.5 46 % Polyethylene glycol 200
0.15 M Citric acid pH 3.5 26 % Polyethylene glycol 200	0.15 M Citric acid pH 3.5 30 % Polyethylene glycol 200	0.15 M Citric acid pH 3.5 34 % Polyethylene glycol 200	0.15 M Citric acid pH 3.5 38 % Polyethylene glycol 200	0.15 M Citric acid pH 3.5 42 % Polyethylene glycol 200	0.15 M Citric acid pH 3.5 46 % Polyethylene glycol 200
0.20 M Citric acid pH 3.5 26 % Polyethylene glycol 200	0.20 M Citric acid pH 3.5 30 % Polyethylene glycol 200	0.20 M Citric acid pH 3.5 34 % Polyethylene glycol 200	0.20 M Citric acid pH 3.5 38 % Polyethylene glycol 200	0.20 M Citric acid pH 3.5 42 % Polyethylene glycol 200	0.20 M Citric acid pH 3.5 46 % Polyethylene glycol 200

Rec/LG (9 mg/mL): Ammonium phosphate dibasic + tris

2.0 M Ammonium phosphate dibasic 0.05 M Tris pH 8.5	2.2 M Ammonium phosphate dibasic 0.05 M Tris pH 8.5	2.4 M Ammonium phosphate dibasic 0.05 M Tris pH 8.5	2.6 M Ammonium phosphate dibasic 0.05 M Tris pH 8.5	2.8 M Ammonium phosphate dibasic 0.05 M Tris pH 8.5	3.0 M Ammonium phosphate dibasic 0.05 M Tris pH 8.5
2.0 M Ammonium phosphate dibasic 0.10 M Tris pH 8.5	2.2 M Ammonium phosphate dibasic 0.10 M Tris pH 8.5	2.4 M Ammonium phosphate dibasic 0.10 M Tris pH 8.5	2.6 M Ammonium phosphate dibasic 0.10 M Tris pH 8.5	2.8 M Ammonium phosphate dibasic 0.10 M Tris pH 8.5	3.0 M Ammonium phosphate dibasic 0.10 M Tris pH 8.5
2.0 M Ammonium phosphate dibasic 0.15 M Tris pH 8.5	2.2 M Ammonium phosphate dibasic 0.15 M Tris pH 8.5	2.4 M Ammonium phosphate dibasic 0.15 M Tris pH 8.5	2.6 M Ammonium phosphate dibasic 0.15 M Tris pH 8.5	2.8 M Ammonium phosphate dibasic 0.15 M Tris pH 8.5	3.0 M Ammonium phosphate dibasic 0.15 M Tris pH 8.5

2.0 M Ammonium phosphate dibasic 0.20 M Tris pH 8.5	2.2 M Ammonium phosphate dibasic 0.20 M Tris pH 8.5	2.4 M Ammonium phosphate dibasic 0.20 M Tris pH 8.5	2.6 M Ammonium phosphate dibasic 0.20 M Tris pH 8.5	2.8 M Ammonium phosphate dibasic 0.20 M Tris pH 8.5	3.0 M Ammonium phosphate dibasic 0.20 M Tris pH 8.5
--	--	--	--	--	--

Rec/LG (68 mg/mL): Lithium sulfate + BIS-TRIS propane

0.9 M Lithium sulphate monohydrate 0.05 M BIS-TRIS propane pH 7	1.1 M Lithium sulphate monohydrate 0.05 M BIS-TRIS propane pH 7	1.3 M Lithium sulphate monohydrate 0.05 M BIS-TRIS propane pH 7	1.5 M Lithium sulphate monohydrate 0.05 M BIS-TRIS propane pH 7	1.7 M Lithium sulphate monohydrate 0.05 M BIS-TRIS propane pH 7	1.9 M Lithium sulphate monohydrate 0.05 M BIS-TRIS propane pH 7
0.9 M Lithium sulphate monohydrate 0.10 M BIS-TRIS propane pH 7	1.1 M Lithium sulphate monohydrate 0.10 M BIS-TRIS propane pH 7	1.3 M Lithium sulphate monohydrate 0.10 M BIS-TRIS propane pH 7	1.5 M Lithium sulphate monohydrate 0.10 M BIS-TRIS propane pH 7	1.7 M Lithium sulphate monohydrate 0.10 M BIS-TRIS propane pH 7	1.9 M Lithium sulphate monohydrate 0.10 M BIS-TRIS propane pH 7
0.9 M Lithium sulphate monohydrate 0.15 M BIS-TRIS propane pH 7	1.1 M Lithium sulphate monohydrate 0.15 M BIS-TRIS propane pH 7	1.3 M Lithium sulphate monohydrate 0.15 M BIS-TRIS propane pH 7	1.5 M Lithium sulphate monohydrate 0.15 M BIS-TRIS propane pH 7	1.7 M Lithium sulphate monohydrate 0.15 M BIS-TRIS propane pH 7	1.9 M Lithium sulphate monohydrate 0.15 M BIS-TRIS propane pH 7
0.9 M Lithium sulphate monohydrate 0.20 M BIS-TRIS propane pH 7	1.1 M Lithium sulphate monohydrate 0.20 M BIS-TRIS propane pH 7	1.3 M Lithium sulphate monohydrate 0.20 M BIS-TRIS propane pH 7	1.5 M Lithium sulphate monohydrate 0.20 M BIS-TRIS propane pH 7	1.7 M Lithium sulphate monohydrate 0.20 M BIS-TRIS propane pH 7	1.9 M Lithium sulphate monohydrate 0.20 M BIS-TRIS propane pH 7

Rec/LG (68 mg/mL): Nickel chloride + lithium sulfate + tris

0.005 M Nickel Chloride 0.6 M Lithium Sulfate 0.1 M Tris pH 8.5	0.005 M Nickel Chloride 0.8 M Lithium Sulfate 0.1 M Tris pH 8.5	0.005 M Nickel Chloride 1.0 M Lithium Sulfate 0.1 M Tris pH 8.5	0.005 M Nickel Chloride 1.2 M Lithium Sulfate 0.1 M Tris pH 8.5	0.005 M Nickel Chloride 1.4 M Lithium Sulfate 0.1 M Tris pH 8.5	0.005 M Nickel Chloride 1.6 M Lithium Sulfate 0.1 M Tris pH 8.5
0.010 M Nickel Chloride 0.6 M Lithium Sulfate 0.1 M Tris pH 8.5	0.010 M Nickel Chloride 0.8 M Lithium Sulfate 0.1 M Tris pH 8.5	0.010 M Nickel Chloride 1.0 M Lithium Sulfate 0.1 M Tris pH 8.5	0.010 M Nickel Chloride 1.2 M Lithium Sulfate 0.1 M Tris pH 8.5	0.010 M Nickel Chloride 1.4 M Lithium Sulfate 0.1 M Tris pH 8.5	0.010 M Nickel Chloride 1.6 M Lithium Sulfate 0.1 M Tris pH 8.5

0.015 M Nickel Chloride 0.6 M Lithium Sulfate 0.1 M Tris pH 8.5	0.015 M Nickel Chloride 0.8 M Lithium Sulfate 0.1 M Tris pH 8.5	0.015 M Nickel Chloride 1.0 M Lithium Sulfate 0.1 M Tris pH 8.5	0.015 M Nickel Chloride 1.2 M Lithium Sulfate 0.1 M Tris pH 8.5	0.015 M Nickel Chloride 1.4 M Lithium Sulfate 0.1 M Tris pH 8.5	0.015 M Nickel Chloride 1.6 M Lithium Sulfate 0.1 M Tris pH 8.5
0.020 M Nickel Chloride 0.6 M Lithium Sulfate 0.1 M Tris pH 8.5	0.020 M Nickel Chloride 0.8 M Lithium Sulfate 0.1 M Tris pH 8.5	0.020 M Nickel Chloride 1.0 M Lithium Sulfate 0.1 M Tris pH 8.5	0.020 M Nickel Chloride 1.2 M Lithium Sulfate 0.1 M Tris pH 8.5	0.020 M Nickel Chloride 1.4 M Lithium Sulfate 0.1 M Tris pH 8.5	0.020 M Nickel Chloride 1.6 M Lithium Sulfate 0.1 M Tris pH 8.5

Rec/LG (68 mg/mL): Ammonium sulfate + glycerol + tris

1.1 M Ammonium Sulfate 8 % Glycerol 0.1 M Tris pH 8.5	1.3 M Ammonium Sulfate 8 % Glycerol 0.1 M Tris pH 8.5	1.5 M Ammonium Sulfate 8 % Glycerol 0.1 M Tris pH 8.5	1.7 M Ammonium Sulfate 8 % Glycerol 0.1 M Tris pH 8.5	1.9 M Ammonium Sulfate 8 % Glycerol 0.1 M Tris pH 8.5	2.1 M Ammonium Sulfate 8 % Glycerol 0.1 M Tris pH 8.5
1.1 M Ammonium Sulfate 10 % Glycerol 0.1 M Tris pH 8.5	1.3 M Ammonium Sulfate 10 % Glycerol 0.1 M Tris pH 8.5	1.5 M Ammonium Sulfate 10 % Glycerol 0.1 M Tris pH 8.5	1.7 M Ammonium Sulfate 10 % Glycerol 0.1 M Tris pH 8.5	1.9 M Ammonium Sulfate 10 % Glycerol 0.1 M Tris pH 8.5	2.1 M Ammonium Sulfate 10 % Glycerol 0.1 M Tris pH 8.5
1.1 M Ammonium Sulfate 12 % Glycerol 0.1 M Tris pH 8.5	1.3 M Ammonium Sulfate 12 % Glycerol 0.1 M Tris pH 8.5	1.5 M Ammonium Sulfate 12 % Glycerol 0.1 M Tris pH 8.5	1.7 M Ammonium Sulfate 12 % Glycerol 0.1 M Tris pH 8.5	1.9 M Ammonium Sulfate 12 % Glycerol 0.1 M Tris pH 8.5	2.1 M Ammonium Sulfate 12 % Glycerol 0.1 M Tris pH 8.5
1.1 M Ammonium Sulfate 14 % Glycerol 0.1 M Tris pH 8.5	1.3 M Ammonium Sulfate 14 % Glycerol 0.1 M Tris pH 8.5	1.5 M Ammonium Sulfate 14 % Glycerol 0.1 M Tris pH 8.5	1.7 M Ammonium Sulfate 14 % Glycerol 0.1 M Tris pH 8.5	1.9 M Ammonium Sulfate 14 % Glycerol 0.1 M Tris pH 8.5	2.1 M Ammonium Sulfate 14 % Glycerol 0.1 M Tris pH 8.5

Rec/LG (68 mg/mL): Calcium chloride + 2-methyl-2,4-pentanediol + BIS-TRIS

0.1 M Calcium chloride dihydrate 35 % 2-Methyl-2,4-pentanediol 0.1 M BIS-TRIS pH 5.9	.1 M Calcium chloride dihydrate 35 % 2-Methyl-2,4-pentanediol 0.1 M BIS-TRIS pH 6.1	.1 M Calcium chloride dihydrate 35 % 2-Methyl-2,4-pentanediol 0.1 M BIS-TRIS pH 6.3	.1 M Calcium chloride dihydrate 35 % 2-Methyl-2,4-pentanediol 0.1 M BIS-TRIS pH 6.5	.1 M Calcium chloride dihydrate 35 % 2-Methyl-2,4-pentanediol 0.1 M BIS-TRIS pH 6.7	.1 M Calcium chloride dihydrate 35 % 2-Methyl-2,4-pentanediol 0.1 M BIS-TRIS pH 6.9
--	---	---	---	---	---

0.015 M Nickel Chloride 0.6 M Lithium Sulfate 0.1 M Tris pH 8.1	0.015 M Nickel Chloride 0.6 M Lithium Sulfate 0.1 M Tris pH 8.3	0.015 M Nickel Chloride 0.6 M Lithium Sulfate 0.1 M Tris pH 8.5	0.015 M Nickel Chloride 0.6 M Lithium Sulfate 0.1 M Tris pH 8.7	0.015 M Nickel Chloride 0.6 M Lithium Sulfate 0.1 M Tris pH 8.9	0.015 M Nickel Chloride 0.6 M Lithium Sulfate 0.1 M Tris pH 9.1
0.05 M BIS-TRIS Propane pH 8.5 14 % Jeffamine pH 7	0.05 M BIS-TRIS Propane pH 8.6 14 % Jeffamine pH 7	0.05 M BIS-TRIS Propane pH 8.8 14 % Jeffamine pH 7	0.05 M BIS-TRIS Propane pH 9.0 14 % Jeffamine pH 7	0.05 M BIS-TRIS Propane pH 9.2 14 % Jeffamine pH 7	0.05 M BIS-TRIS Propane pH 9.5 14 % Jeffamine pH 7
1.1 M Ammonium Sulfate 8 % Glycerol 0.1 M Tris pH 8.5	1.1 M Ammonium Sulfate 8 % Glycerol 0.1 M Tris pH 8.5	1.1 M Ammonium Sulfate 8 % Glycerol 0.1 M Tris pH 8.5	1.1 M Ammonium Sulfate 8 % Glycerol 0.1 M Tris pH 8.5	1.1 M Ammonium Sulfate 8 % Glycerol 0.1 M Tris pH 8.5	1.1 M Ammonium Sulfate 8 % Glycerol 0.1 M Tris pH 8.5

Rec/LG (50 mg/mL): Sodium chloride + sodium acetate + MPD

0.10 M NaCl 0.05 M Sodium Acetate Trihydrate pH 4.8 30 % MPD	0.15 M NaCl 0.05 M Sodium Acetate Trihydrate pH 4.8 30 % MPD	0.20 M NaCl 0.05 M Sodium Acetate Trihydrate pH 4.8 30 % MPD	0.25 M NaCl 0.05 M Sodium Acetate Trihydrate pH 4.8 30 % MPD	0.30 M NaCl 0.05 M Sodium Acetate Trihydrate pH 4.8 30 % MPD	0.35 M NaCl 0.05 M Sodium Acetate Trihydrate pH 4.8 30 % MPD
0.10 M NaCl 0.10 M Sodium Acetate Trihydrate pH 4.8 30 % MPD	0.15 M NaCl 0.10 M Sodium Acetate Trihydrate pH 4.8 30 % MPD	0.20 M NaCl 0.10 M Sodium Acetate Trihydrate pH 4.8 30 % MPD	0.25 M NaCl 0.10 M Sodium Acetate Trihydrate pH 4.8 30 % MPD	0.30 M NaCl 0.10 M Sodium Acetate Trihydrate pH 4.8 30 % MPD	0.35 M NaCl 0.10 M Sodium Acetate Trihydrate pH 4.8 30 % MPD
0.10 M NaCl 0.15 M Sodium Acetate Trihydrate pH 4.8 30 % MPD	0.15 M NaCl 0.15 M Sodium Acetate Trihydrate pH 4.8 30 % MPD	0.20 M NaCl 0.15 M Sodium Acetate Trihydrate pH 4.8 30 % MPD	0.25 M NaCl 0.15 M Sodium Acetate Trihydrate pH 4.8 30 % MPD	0.30 M NaCl 0.15 M Sodium Acetate Trihydrate pH 4.8 30 % MPD	0.35 M NaCl 0.15 M Sodium Acetate Trihydrate pH 4.8 30 % MPD
0.10 M NaCl 0.20 M Sodium Acetate Trihydrate pH 4.8 30 % MPD	0.15 M NaCl 0.20 M Sodium Acetate Trihydrate pH 4.8 30 % MPD	0.20 M NaCl 0.20 M Sodium Acetate Trihydrate pH 4.8 30 % MPD	0.25 M NaCl 0.20 M Sodium Acetate Trihydrate pH 4.8 30 % MPD	0.30 M NaCl 0.20 M Sodium Acetate Trihydrate pH 4.8 30 % MPD	0.35 M NaCl 0.20 M Sodium Acetate Trihydrate pH 4.8 30 % MPD

Rec/LG (46 mg/mL): Ammonium nitrate + tris

4.5 M Ammonium Nitrate 0.05 M Tris pH 8.5	5.0 M Ammonium Nitrate 0.05 M Tris pH 8.5	5.5 M Ammonium Nitrate 0.05 M Tris pH 8.5	6.0 M Ammonium Nitrate 0.05 M Tris pH 8.5	6.5 M Ammonium Nitrate 0.05 M Tris pH 8.5	7.0 M Ammonium Nitrate 0.05 M Tris pH 8.5
4.5 M Ammonium Nitrate 0.10 M Tris pH 8.5	5.0 M Ammonium Nitrate 0.10 M Tris pH 8.5	5.5 M Ammonium Nitrate 0.10 M Tris pH 8.5	6.0 M Ammonium Nitrate 0.10 M Tris pH 8.5	6.5 M Ammonium Nitrate 0.10 M Tris pH 8.5	7.0 M Ammonium Nitrate 0.10 M Tris pH 8.5
4.5 M Ammonium Nitrate 0.15 M Tris pH 8.5	5.0 M Ammonium Nitrate 0.15 M Tris pH 8.5	5.5 M Ammonium Nitrate 0.15 M Tris pH 8.5	6.0 M Ammonium Nitrate 0.15 M Tris pH 8.5	6.5 M Ammonium Nitrate 0.15 M Tris pH 8.5	7.0 M Ammonium Nitrate 0.15 M Tris pH 8.5
4.5 M Ammonium Nitrate 0.20 M Tris pH 8.5	5.0 M Ammonium Nitrate 0.20 M Tris pH 8.5	5.5 M Ammonium Nitrate 0.20 M Tris pH 8.5	6.0 M Ammonium Nitrate 0.20 M Tris pH 8.5	6.5 M Ammonium Nitrate 0.20 M Tris pH 8.5	7.0 M Ammonium Nitrate 0.20 M Tris pH 8.5

Rec/LG (46 mg/mL): Sodium formate + BICINE

0.10 M Sodium Formate 0.05 M BICINE pH 8.5 20 % PEG 5000	0.15 M Sodium Formate 0.05 M BICINE pH 8.5 20 % PEG 5000	0.20 M Sodium Formate 0.05 M BICINE pH 8.5 20 % PEG 5000	0.25 M Sodium Formate 0.05 M BICINE pH 8.5 20 % PEG 5000	0.30 M Sodium Formate 0.05 M BICINE pH 8.5 20 % PEG 5000	0.35 M Sodium Formate 0.05 M BICINE pH 8.5 20 % PEG 5000
0.10 M Sodium Formate 0.10 M BICINE pH 8.5 20 % PEG 5000	0.15 M Sodium Formate 0.10 M BICINE pH 8.5 20 % PEG 5000	0.20 M Sodium Formate 0.10 M BICINE pH 8.5 20 % PEG 5000	0.25 M Sodium Formate 0.10 M BICINE pH 8.5 20 % PEG 5000	0.30 M Sodium Formate 0.10 M BICINE pH 8.5 20 % PEG 5000	0.35 M Sodium Formate 0.10 M BICINE pH 8.5 20 % PEG 5000
0.10 M Sodium Formate 0.15 M BICINE pH 8.5 20 % PEG 5000	0.15 M Sodium Formate 0.15 M BICINE pH 8.5 20 % PEG 5000	0.20 M Sodium Formate 0.15 M BICINE pH 8.5 20 % PEG 5000	0.25 M Sodium Formate 0.15 M BICINE pH 8.5 20 % PEG 5000	0.30 M Sodium Formate 0.15 M BICINE pH 8.5 20 % PEG 5000	0.35 M Sodium Formate 0.15 M BICINE pH 8.5 20 % PEG 5000
0.10 M Sodium Formate 0.20 M BICINE pH 8.5 20 % PEG 5000	0.15 M Sodium Formate 0.20 M BICINE pH 8.5 20 % PEG 5000	0.20 M Sodium Formate 0.20 M BICINE pH 8.5 20 % PEG 5000	0.25 M Sodium Formate 0.20 M BICINE pH 8.5 20 % PEG 5000	0.30 M Sodium Formate 0.20 M BICINE pH 8.5 20 % PEG 5000	0.35 M Sodium Formate 0.20 M BICINE pH 8.5 20 % PEG 5000

Rec/LG (46 mg/mL): Nickel chloride + tris + lithium sulfate

0.005 M Nickel Chloride 0.6 M Lithium Sulfate 0.1 M Tris pH 8.5	0.005 M Nickel Chloride 0.8 M Lithium Sulfate 0.1 M Tris pH 8.5	0.005 M Nickel Chloride 1.0 M Lithium Sulfate 0.1 M Tris pH 8.5	0.005 M Nickel Chloride 1.2 M Lithium Sulfate 0.1 M Tris pH 8.5	0.005 M Nickel Chloride 1.4 M Lithium Sulfate 0.1 M Tris pH 8.5	0.005 M Nickel Chloride 1.6 M Lithium Sulfate 0.1 M Tris pH 8.5
0.010 M Nickel Chloride 0.6 M Lithium Sulfate 0.1 M Tris pH 8.5	0.010 M Nickel Chloride 0.8 M Lithium Sulfate 0.1 M Tris pH 8.5	0.010 M Nickel Chloride 1.0 M Lithium Sulfate 0.1 M Tris pH 8.5	0.010 M Nickel Chloride 1.2 M Lithium Sulfate 0.1 M Tris pH 8.5	0.010 M Nickel Chloride 1.4 M Lithium Sulfate 0.1 M Tris pH 8.5	0.010 M Nickel Chloride 1.6 M Lithium Sulfate 0.1 M Tris pH 8.5
0.015 M Nickel Chloride 0.6 M Lithium Sulfate 0.1 M Tris pH 8.5	0.015 M Nickel Chloride 0.8 M Lithium Sulfate 0.1 M Tris pH 8.5	0.015 M Nickel Chloride 1.0 M Lithium Sulfate 0.1 M Tris pH 8.5	0.015 M Nickel Chloride 1.2 M Lithium Sulfate 0.1 M Tris pH 8.5	0.015 M Nickel Chloride 1.4 M Lithium Sulfate 0.1 M Tris pH 8.5	0.015 M Nickel Chloride 1.6 M Lithium Sulfate 0.1 M Tris pH 8.5
0.020 M Nickel Chloride 0.6 M Lithium Sulfate 0.1 M Tris pH 8.5	0.020 M Nickel Chloride 0.8 M Lithium Sulfate 0.1 M Tris pH 8.5	0.020 M Nickel Chloride 1.0 M Lithium Sulfate 0.1 M Tris pH 8.5	0.020 M Nickel Chloride 1.2 M Lithium Sulfate 0.1 M Tris pH 8.5	0.020 M Nickel Chloride 1.4 M Lithium Sulfate 0.1 M Tris pH 8.5	0.020 M Nickel Chloride 1.6 M Lithium Sulfate 0.1 M Tris pH 8.5

Rec/LG (46 mg/mL): Ammonium sulfate + tris + glycerol

0.9 M Ammonium Sulfate 0.05 M Tris pH 8.5 12 % Glycerol	1.1 M Ammonium Sulfate 0.05 M Tris pH 8.5 12 % Glycerol	1.3 M Ammonium Sulfate 0.05 M Tris pH 8.5 12 % Glycerol	1.5 M Ammonium Sulfate 0.05 M Tris pH 8.5 12 % Glycerol	1.7 M Ammonium Sulfate 0.05 M Tris pH 8.5 12 % Glycerol	1.9 M Ammonium Sulfate 0.05 M Tris pH 8.5 12 % Glycerol
0.9 M Ammonium Sulfate 0.10 M Tris pH 8.5 12 % Glycerol	1.1 M Ammonium Sulfate 0.10 M Tris pH 8.5 12 % Glycerol	1.3 M Ammonium Sulfate 0.10 M Tris pH 8.5 12 % Glycerol	1.5 M Ammonium Sulfate 0.10 M Tris pH 8.5 12 % Glycerol	1.7 M Ammonium Sulfate 0.10 M Tris pH 8.5 12 % Glycerol	1.9 M Ammonium Sulfate 0.10 M Tris pH 8.5 12 % Glycerol
0.9 M Ammonium Sulfate 0.15 M Tris pH 8.5 12 % Glycerol	1.1 M Ammonium Sulfate 0.15 M Tris pH 8.5 12 % Glycerol	1.3 M Ammonium Sulfate 0.15 M Tris pH 8.5 12 % Glycerol	1.5 M Ammonium Sulfate 0.15 M Tris pH 8.5 12 % Glycerol	1.7 M Ammonium Sulfate 0.15 M Tris pH 8.5 12 % Glycerol	1.9 M Ammonium Sulfate 0.15 M Tris pH 8.5 12 % Glycerol

0.9 M Ammonium Sulfate 0.20 M Tris pH 8.5 12 % Glycerol	1.1 M Ammonium Sulfate 0.20 M Tris pH 8.5 12 % Glycerol	1.3 M Ammonium Sulfate 0.20 M Tris pH 8.5 12 % Glycerol	1.5 M Ammonium Sulfate 0.20 M Tris pH 8.5 12 % Glycerol	1.7 M Ammonium Sulfate 0.20 M Tris pH 8.5 12 % Glycerol	1.9 M Ammonium Sulfate 0.20 M Tris pH 8.5 12 % Glycerol
---	---	---	---	---	---

Rec/EX (29 mg/mL + IPM): HEPES + PEG 8000 + Ethylene glycol

0.1 M HEPES pH 8.4 10 % PEG 8000 4 % Ethylene Glycol	0.1 M HEPES pH 8.6 10 % PEG 8000 4 % Ethylene Glycol	0.1 M HEPES pH 8.8 10 % PEG 8000 4 % Ethylene Glycol	0.1 M HEPES pH 9.0 10 % PEG 8000 4 % Ethylene Glycol	0.1 M HEPES pH 9.2 10 % PEG 8000 4 % Ethylene Glycol	0.1 M HEPES pH 9.4 10 % PEG 8000 4 % Ethylene Glycol
0.1 M HEPES pH 8.4 10 % PEG 8000 6 % Ethylene Glycol	0.1 M HEPES pH 8.6 10 % PEG 8000 6 % Ethylene Glycol	0.1 M HEPES pH 8.8 10 % PEG 8000 6 % Ethylene Glycol	0.1 M HEPES pH 9.0 10 % PEG 8000 6 % Ethylene Glycol	0.1 M HEPES pH 9.2 10 % PEG 8000 6 % Ethylene Glycol	0.1 M HEPES pH 9.4 10 % PEG 8000 6 % Ethylene Glycol
0.1 M HEPES 10 % PEG 8000 8 % Ethylene Glycol	0.1 M HEPES pH 8.6 10 % PEG 8000 8 % Ethylene Glycol	0.1 M HEPES pH 8.8 10 % PEG 8000 8 % Ethylene Glycol	0.1 M HEPES pH 9.0 10 % PEG 8000 8 % Ethylene Glycol	0.1 M HEPES 10 % PEG 8000 8 % Ethylene Glycol	0.1 M HEPES pH 9.4 10 % PEG 8000 8 % Ethylene Glycol
0.1 M HEPES 10 % PEG 8000 10 % Ethylene Glycol	0.1 M HEPES pH 8.6 10 % PEG 8000 10 % Ethylene Glycol	0.1 M HEPES pH 8.8 10 % PEG 8000 10 % Ethylene Glycol	0.1 M HEPES pH 9.0 10 % PEG 8000 10 % Ethylene Glycol	0.1 M HEPES 10 % PEG 8000 10 % Ethylene Glycol	0.1 M HEPES pH 9.4 10 % PEG 8000 10 % Ethylene Glycol

Rec/EX (29 mg/mL + IPM): BIS-TRIS propane + PEG 550

0.1 M BIS-TRIS Propane 15 % PEG 550					
0.1 M BIS-TRIS Propane 20 % PEG 550					

0.1 M BIS-TRIS Propane 25 % PEG 550					
0.1 M BIS-TRIS Propane 30 % PEG 550					

**Rec/EX (33 mg/mL): MPD + HEPES + PEG 10,000**

5 % MPD 0.05 M HEPES pH 6.9 10 % PEG 10000	5 % MPD 0.05 M HEPES pH 7.1 10 % PEG 10000	5 % MPD 0.05 M HEPES pH 7.3 10 % PEG 10000	5 % MPD 0.05 M HEPES pH 7.5 10 % PEG 10000	5 % MPD 0.05 M HEPES pH 7.7 10 % PEG 10000	5 % MPD 0.05 M HEPES pH 7.9 10 % PEG 10000
5 % MPD 0.10 M HEPES pH 6.9 10 % PEG 10000	5 % MPD 0.10 M HEPES pH 7.1 10 % PEG 10000	5 % MPD 0.10 M HEPES pH 7.3 10 % PEG 10000	5 % MPD 0.10 M HEPES pH 7.5 10 % PEG 10000	5 % MPD 0.10 M HEPES pH 7.7 10 % PEG 10000	5 % MPD 0.10 M HEPES pH 7.9 10 % PEG 10000
5 % MPD 0.15 M HEPES pH 6.9 10 % PEG 10000	5 % MPD 0.15 M HEPES pH 7.1 10 % PEG 10000	5 % MPD 0.15 M HEPES pH 7.3 10 % PEG 10000	5 % MPD 0.15 M HEPES pH 7.5 10 % PEG 10000	5 % MPD 0.15 M HEPES pH 7.7 10 % PEG 10000	5 % MPD 0.15 M HEPES pH 7.9 10 % PEG 10000
5 % MPD 0.20 M HEPES pH 6.9 10 % PEG 10000	5 % MPD 0.20 M HEPES pH 7.1 10 % PEG 10000	5 % MPD 0.20 M HEPES pH 7.3 10 % PEG 10000	5 % MPD 0.20 M HEPES pH 7.5 10 % PEG 10000	5 % MPD 0.20 M HEPES pH 7.7 10 % PEG 10000	5 % MPD 0.20 M HEPES pH 7.9 10 % PEG 10000

**Rec/EX (33 mg/mL): Sodium chloride + BIS-TRIS propane**

2.6 M Sodium Chloride 0.05 M BIS-TRIS propane pH 7	2.8 M Sodium Chloride 0.05 M BIS-TRIS propane pH 7	3.0 M Sodium Chloride 0.05 M BIS-TRIS propane pH 7	3.2 M Sodium Chloride 0.05 M BIS-TRIS propane pH 7	3.4 M Sodium Chloride 0.05 M BIS-TRIS propane pH 7	3.6 M Sodium Chloride 0.05 M BIS-TRIS propane pH 7
--	--	--	--	--	--

2.6 M Sodium Chloride 0.10 M BIS-TRIS propane pH 7	2.8 M Sodium Chloride 0.10 M BIS-TRIS propane pH 7	3.0 M Sodium Chloride 0.10 M BIS-TRIS propane pH 7	3.2 M Sodium Chloride 0.10 M BIS-TRIS propane pH 7	3.4 M Sodium Chloride 0.10 M BIS-TRIS propane pH 7	3.6 M Sodium Chloride 0.10 M BIS-TRIS propane pH 7
2.6 M Sodium Chloride 0.15 M BIS-TRIS propane pH 7	2.8 M Sodium Chloride 0.15 M BIS-TRIS propane pH 7	3.0 M Sodium Chloride 0.15 M BIS-TRIS propane pH 7	3.2 M Sodium Chloride 0.15 M BIS-TRIS propane pH 7	3.4 M Sodium Chloride 0.15 M BIS-TRIS propane pH 7	3.6 M Sodium Chloride 0.15 M BIS-TRIS propane pH 7
2.6 M Sodium Chloride 0.20 M BIS-TRIS propane pH 7	2.8 M Sodium Chloride 0.20 M BIS-TRIS propane pH 7	3.0 M Sodium Chloride 0.20 M BIS-TRIS propane pH 7	3.2 M Sodium Chloride 0.20 M BIS-TRIS propane pH 7	3.4 M Sodium Chloride 0.20 M BIS-TRIS propane pH 7	3.6 M Sodium Chloride 0.20 M BIS-TRIS propane pH 7

Rec/EX (33 mg/mL): BIS-TRIS + PEG 1500

0.02 M BIS-TRIS pH 6.5 16 % PEG 1500	0.06 M BIS-TRIS pH 6.5 16 % PEG 1500	0.10 M BIS-TRIS pH 6.5 16 % PEG 1500	0.14 M BIS-TRIS pH 6.5 16 % PEG 1500	0.18 M BIS-TRIS pH 6.5 16 % PEG 1500	0.22 M BIS-TRIS pH 6.5 16 % PEG 1500
0.02 M BIS-TRIS pH 6.5 18 % PEG 1500	0.06 M BIS-TRIS pH 6.5 18 % PEG 1500	0.10 M BIS-TRIS pH 6.5 18 % PEG 1500	0.14 M BIS-TRIS pH 6.5 18 % PEG 1500	0.18 M BIS-TRIS pH 6.5 18 % PEG 1500	0.22 M BIS-TRIS pH 6.5 18 % PEG 1500
0.02 M BIS-TRIS pH 6.5 20 % PEG 1500	0.06 M BIS-TRIS pH 6.5 20 % PEG 1500	0.10 M BIS-TRIS pH 6.5 20 % PEG 1500	0.14 M BIS-TRIS pH 6.5 20 % PEG 1500	0.18 M BIS-TRIS pH 6.5 20 % PEG 1500	0.22 M BIS-TRIS pH 6.5 20 % PEG 1500
0.02 M BIS-TRIS pH 6.5 22 % PEG 1500	0.06 M BIS-TRIS pH 6.5 22 % PEG 1500	0.10 M BIS-TRIS pH 6.5 22 % PEG 1500	0.14 M BIS-TRIS pH 6.5 22 % PEG 1500	0.18 M BIS-TRIS pH 6.5 22 % PEG 1500	0.22 M BIS-TRIS pH 6.5 22 % PEG 1500

Rec/EX (86 mg/mL): Sodium chloride + sodium acetate + MPD

0.10 M NaCl 0.05 M Sodium Acetate Trihydrate pH 4.8 30 % MPD	0.15 M NaCl 0.05 M Sodium Acetate Trihydrate pH 4.8 30 % MPD	0.20 M NaCl 0.05 M Sodium Acetate Trihydrate pH 4.8 30 % MPD	0.25 M NaCl 0.05 M Sodium Acetate Trihydrate pH 4.8 30 % MPD	0.30 M NaCl 0.05 M Sodium Acetate Trihydrate pH 4.8 30 % MPD	0.35 M NaCl 0.05 M Sodium Acetate Trihydrate pH 4.8 30 % MPD
0.10 M NaCl 0.10 M Sodium Acetate Trihydrate pH 4.8 30 % MPD	0.15 M NaCl 0.10 M Sodium Acetate Trihydrate pH 4.8 30 % MPD	0.20 M NaCl 0.10 M Sodium Acetate Trihydrate pH 4.8 30 % MPD	0.25 M NaCl 0.10 M Sodium Acetate Trihydrate pH 4.8 30 % MPD	0.30 M NaCl 0.10 M Sodium Acetate Trihydrate pH 4.8 30 % MPD	0.35 M NaCl 0.10 M Sodium Acetate Trihydrate pH 4.8 30 % MPD
0.10 M NaCl 0.15 M Sodium Acetate Trihydrate pH 4.8 30 % MPD	0.15 M NaCl 0.15 M Sodium Acetate Trihydrate pH 4.8 30 % MPD	0.20 M NaCl 0.15 M Sodium Acetate Trihydrate pH 4.8 30 % MPD	0.25 M NaCl 0.15 M Sodium Acetate Trihydrate pH 4.8 30 % MPD	0.30 M NaCl 0.15 M Sodium Acetate Trihydrate pH 4.8 30 % MPD	0.35 M NaCl 0.15 M Sodium Acetate Trihydrate pH 4.8 30 % MPD
0.10 M NaCl 0.20 M Sodium Acetate Trihydrate pH 4.8 30 % MPD	0.15 M NaCl 0.20 M Sodium Acetate Trihydrate pH 4.8 30 % MPD	0.20 M NaCl 0.20 M Sodium Acetate Trihydrate pH 4.8 30 % MPD	0.25 M NaCl 0.20 M Sodium Acetate Trihydrate pH 4.8 30 % MPD	0.30 M NaCl 0.20 M Sodium Acetate Trihydrate pH 4.8 30 % MPD	0.35 M NaCl 0.20 M Sodium Acetate Trihydrate pH 4.8 30 % MPD

Rec/EX (69 mg/mL): Diammonium hydrogen citrate + magnesium sulfate + PEG 3350 + glycerol

0.05 M Diammonium Hydrogen Citrate pH 5.5 0.002 M Magnesium Sulfate 15 % PEG 3350 4 % Glycerol	0.10 M Diammonium Hydrogen Citrate pH 5.5 0.002 M Magnesium Sulfate 15 % PEG 3350 4 % Glycerol	0.15 M Diammonium Hydrogen Citrate pH 5.5 0.002 M Magnesium Sulfate 15 % PEG 3350 4 % Glycerol	0.20 M Diammonium Hydrogen Citrate pH 5.5 0.002 M Magnesium Sulfate 15 % PEG 3350 4 % Glycerol	0.25 M Diammonium Hydrogen Citrate pH 5.5 0.002 M Magnesium Sulfate 15 % PEG 3350 4 % Glycerol	0.30 M Diammonium Hydrogen Citrate pH 5.5 0.002 M Magnesium Sulfate 15 % PEG 3350 4 % Glycerol
0.05 M Diammonium Hydrogen Citrate pH 5.5 0.004 M Magnesium Sulfate 15 % PEG 3350 4 % Glycerol	0.10 M Diammonium Hydrogen Citrate pH 5.5 0.004 M Magnesium Sulfate 15 % PEG 3350 4 % Glycerol	0.15 M Diammonium Hydrogen Citrate pH 5.5 0.004 M Magnesium Sulfate 15 % PEG 3350 4 % Glycerol	0.20 M Diammonium Hydrogen Citrate pH 5.5 0.004 M Magnesium Sulfate 15 % PEG 3350 4 % Glycerol	0.25 M Diammonium Hydrogen Citrate pH 5.5 0.004 M Magnesium Sulfate 15 % PEG 3350 4 % Glycerol	0.30 M Diammonium Hydrogen Citrate pH 5.5 0.004 M Magnesium Sulfate 15 % PEG 3350 4 % Glycerol
0.05 M Diammonium Hydrogen Citrate pH 5.5 0.006 M Magnesium Sulfate	0.10 M Diammonium Hydrogen Citrate pH 5.5 0.006 M Magnesium Sulfate	0.15 M Diammonium Hydrogen Citrate pH 5.5 0.006 M Magnesium Sulfate	0.20 M Diammonium Hydrogen Citrate pH 5.5 0.006 M Magnesium Sulfate	0.25 M Diammonium Hydrogen Citrate pH 5.5 0.006 M Magnesium Sulfate	0.30 M Diammonium Hydrogen Citrate pH 5.5 0.006 M Magnesium Sulfate

15 % PEG 3350 4 % Glycerol					
0.05 M Diammonium Hydrogen Citrate pH 5.5 0.008 M Magnesium Sulfate 15 % PEG 3350 4 % Glycerol	0.10 M Diammonium Hydrogen Citrate pH 5.5 0.008 M Magnesium Sulfate 15 % PEG 3350 4 % Glycerol	0.15 M Diammonium Hydrogen Citrate pH 5.5 0.008 M Magnesium Sulfate 15 % PEG 3350 4 % Glycerol	0.20 M Diammonium Hydrogen Citrate pH 5.5 0.008 M Magnesium Sulfate 15 % PEG 3350 4 % Glycerol	0.25 M Diammonium Hydrogen Citrate pH 5.5 0.008 M Magnesium Sulfate 15 % PEG 3350 4 % Glycerol	0.30 M Diammonium Hydrogen Citrate pH 5.5 0.008 M Magnesium Sulfate 15 % PEG 3350 4 % Glycerol

Rec/EX (69 mg/mL): Calcium chloride + 2-methyl-2,4-pentanediol + BIS-TRIS

0.1 M Calcium chloride dihydrate 35 % 2-Methyl-2,4-pentanediol 0.1 M BIS-TRIS pH 5.9	.1 M Calcium chloride dihydrate 35 % 2-Methyl-2,4-pentanediol 0.1 M BIS-TRIS pH 6.1	.1 M Calcium chloride dihydrate 35 % 2-Methyl-2,4-pentanediol 0.1 M BIS-TRIS pH 6.3	.1 M Calcium chloride dihydrate 35 % 2-Methyl-2,4-pentanediol 0.1 M BIS-TRIS pH 6.5	.1 M Calcium chloride dihydrate 35 % 2-Methyl-2,4-pentanediol 0.1 M BIS-TRIS pH 6.7	.1 M Calcium chloride dihydrate 35 % 2-Methyl-2,4-pentanediol 0.1 M BIS-TRIS pH 6.9
0.015 M Nickel Chloride 0.6 M Lithium Sulfate 0.1 M Tris pH 8.1	0.015 M Nickel Chloride 0.6 M Lithium Sulfate 0.1 M Tris pH 8.3	0.015 M Nickel Chloride 0.6 M Lithium Sulfate 0.1 M Tris pH 8.5	0.015 M Nickel Chloride 0.6 M Lithium Sulfate 0.1 M Tris pH 8.7	0.015 M Nickel Chloride 0.6 M Lithium Sulfate 0.1 M Tris pH 8.9	0.015 M Nickel Chloride 0.6 M Lithium Sulfate 0.1 M Tris pH 9.1
0.05 M BIS-TRIS Propane pH 8.5 14 % Jeffamine pH 7	0.05 M BIS-TRIS Propane pH 8.6 14 % Jeffamine pH 7	0.05 M BIS-TRIS Propane pH 8.8 14 % Jeffamine pH 7	0.05 M BIS-TRIS Propane pH 9.0 14 % Jeffamine pH 7	0.05 M BIS-TRIS Propane pH 9.2 14 % Jeffamine pH 7	0.05 M BIS-TRIS Propane pH 9.5 14 % Jeffamine pH 7
1.1 M Ammonium Sulfate 8 % Glycerol 0.1 M Tris pH 8.5	1.1 M Ammonium Sulfate 8 % Glycerol 0.1 M Tris pH 8.5	1.1 M Ammonium Sulfate 8 % Glycerol 0.1 M Tris pH 8.5	1.1 M Ammonium Sulfate 8 % Glycerol 0.1 M Tris pH 8.5	1.1 M Ammonium Sulfate 8 % Glycerol 0.1 M Tris pH 8.5	1.1 M Ammonium Sulfate 8 % Glycerol 0.1 M Tris pH 8.5

Rec/EX (4 mg/mL): BIS-TRIS propane + jeffamine

0.05 M BIS-TRIS Propane pH 9.0 6 % Jeffamine pH 7	0.05 M BIS-TRIS Propane pH 9.0 8 % Jeffamine pH 7	0.05 M BIS-TRIS Propane pH 9.0 10 % Jeffamine pH 7	0.05 M BIS-TRIS Propane pH 9.0 12 % Jeffamine pH 7	0.05 M BIS-TRIS Propane pH 9.0 14 % Jeffamine pH 7	0.05 M BIS-TRIS Propane pH 9.0 16 % Jeffamine pH 7
--	--	---	---	---	---

0.10 M BIS-TRIS Propane pH 9.0 6 % Jeffamine pH 7	0.10 M BIS-TRIS Propane pH 9.0 8 % Jeffamine pH 7	0.10 M BIS-TRIS Propane pH 9.0 10 % Jeffamine pH 7	0.10 M BIS-TRIS Propane pH 9.0 12 % Jeffamine pH 7	0.10 M BIS-TRIS Propane pH 9.0 14 % Jeffamine pH 7	0.10 M BIS-TRIS Propane pH 9.0 16 % Jeffamine pH 7
0.15 M BIS-TRIS Propane pH 9.0 6 % Jeffamine pH 7	0.15 M BIS-TRIS Propane pH 9.0 8 % Jeffamine pH 7	0.15 M BIS-TRIS Propane pH 9.0 10 % Jeffamine pH 7	0.15 M BIS-TRIS Propane pH 9.0 12 % Jeffamine pH 7	0.15 M BIS-TRIS Propane pH 9.0 14 % Jeffamine pH 7	0.15 M BIS-TRIS Propane pH 9.0 16 % Jeffamine pH 7
0.20 M BIS-TRIS Propane pH 9.0 6 % Jeffamine pH 7	0.20 M BIS-TRIS Propane pH 9.0 8 % Jeffamine pH 7	0.20 M BIS-TRIS Propane pH 9.0 10 % Jeffamine pH 7	0.20 M BIS-TRIS Propane pH 9.0 12 % Jeffamine pH 7	0.20 M BIS-TRIS Propane pH 9.0 14 % Jeffamine pH 7	0.20 M BIS-TRIS Propane pH 9.0 16 % Jeffamine pH 7

Rec/EX (4 mg/mL): Calcium chloride + 2-methyl-2,4-pentanediol + BIS-TRIS

0.1 M Calcium chloride dihydrate 35 % 2-Methyl-2,4-pentanediol 0.1 M BIS-TRIS	0.1 M Calcium chloride dihydrate 40 % 2-Methyl-2,4-pentanediol 0.1 M BIS-TRIS	0.1 M Calcium chloride dihydrate 45 % 2-Methyl-2,4-pentanediol 0.1 M BIS-TRIS	0.1 M Calcium chloride dihydrate 50 % 2-Methyl-2,4-pentanediol 0.1 M BIS-TRIS	0.1 M Calcium chloride dihydrate 55 % 2-Methyl-2,4-pentanediol 0.1 M BIS-TRIS	0.1 M Calcium chloride dihydrate 60 % 2-Methyl-2,4-pentanediol 0.1 M BIS-TRIS
0.2 M Calcium chloride dihydrate 35 % 2-Methyl-2,4-pentanediol 0.1 M BIS-TRIS	0.2 M Calcium chloride dihydrate 40 % 2-Methyl-2,4-pentanediol 0.1 M BIS-TRIS	0.2 M Calcium chloride dihydrate 45 % 2-Methyl-2,4-pentanediol 0.1 M BIS-TRIS	0.2 M Calcium chloride dihydrate 50 % 2-Methyl-2,4-pentanediol 0.1 M BIS-TRIS	0.2 M Calcium chloride dihydrate 55 % 2-Methyl-2,4-pentanediol 0.1 M BIS-TRIS	0.2 M Calcium chloride dihydrate 60 % 2-Methyl-2,4-pentanediol 0.1 M BIS-TRIS
0.3 M Calcium chloride dihydrate 35 % 2-Methyl-2,4-pentanediol 0.1 M BIS-TRIS	0.3 M Calcium chloride dihydrate 40 % 2-Methyl-2,4-pentanediol 0.1 M BIS-TRIS	0.3 M Calcium chloride dihydrate 45 % 2-Methyl-2,4-pentanediol 0.1 M BIS-TRIS	0.3 M Calcium chloride dihydrate 50 % 2-Methyl-2,4-pentanediol 0.1 M BIS-TRIS	0.3 M Calcium chloride dihydrate 55 % 2-Methyl-2,4-pentanediol 0.1 M BIS-TRIS	0.3 M Calcium chloride dihydrate 60 % 2-Methyl-2,4-pentanediol 0.1 M BIS-TRIS
0.4 M Calcium chloride dihydrate 35 % 2-Methyl-2,4-pentanediol 0.1 M BIS-TRIS	0.4 M Calcium chloride dihydrate 40 % 2-Methyl-2,4-pentanediol 0.1 M BIS-TRIS	0.4 M Calcium chloride dihydrate 45 % 2-Methyl-2,4-pentanediol 0.1 M BIS-TRIS	0.4 M Calcium chloride dihydrate 50 % 2-Methyl-2,4-pentanediol 0.1 M BIS-TRIS	0.4 M Calcium chloride dihydrate 55 % 2-Methyl-2,4-pentanediol 0.1 M BIS-TRIS	0.4 M Calcium chloride dihydrate 60 % 2-Methyl-2,4-pentanediol 0.1 M BIS-TRIS

Rec/EX (4 mg/mL): Ammonium phosphate + tris

2.0 M Ammonium phosphate dibasic 0.05 M Tris pH 8.5	2.2 M Ammonium phosphate dibasic 0.05 M Tris pH 8.5	2.4 M Ammonium phosphate dibasic 0.05 M Tris pH 8.5	2.6 M Ammonium phosphate dibasic 0.05 M Tris pH 8.5	2.8 M Ammonium phosphate dibasic 0.05 M Tris pH 8.5	3.0 M Ammonium phosphate dibasic 0.05 M Tris pH 8.5
2.0 M Ammonium phosphate dibasic 0.10 M Tris pH 8.5	2.2 M Ammonium phosphate dibasic 0.10 M Tris pH 8.5	2.4 M Ammonium phosphate dibasic 0.10 M Tris pH 8.5	2.6 M Ammonium phosphate dibasic 0.10 M Tris pH 8.5	2.8 M Ammonium phosphate dibasic 0.10 M Tris pH 8.5	3.0 M Ammonium phosphate dibasic 0.10 M Tris pH 8.5
2.0 M Ammonium phosphate dibasic 0.15 M Tris pH 8.5	2.2 M Ammonium phosphate dibasic 0.15 M Tris pH 8.5	2.4 M Ammonium phosphate dibasic 0.15 M Tris pH 8.5	2.6 M Ammonium phosphate dibasic 0.15 M Tris pH 8.5	2.8 M Ammonium phosphate dibasic 0.15 M Tris pH 8.5	3.0 M Ammonium phosphate dibasic 0.15 M Tris pH 8.5
2.0 M Ammonium phosphate dibasic 0.20 M Tris pH 8.5	2.2 M Ammonium phosphate dibasic 0.20 M Tris pH 8.5	2.4 M Ammonium phosphate dibasic 0.20 M Tris pH 8.5	2.6 M Ammonium phosphate dibasic 0.20 M Tris pH 8.5	2.8 M Ammonium phosphate dibasic 0.20 M Tris pH 8.5	3.0 M Ammonium phosphate dibasic 0.20 M Tris pH 8.5

Rec/EX (4 mg/mL): Citric acid + PEG 200

0.05 M Citric acid pH 3.5 26 % Polyethylene glycol 200	0.05 M Citric acid pH 3.5 30 % Polyethylene glycol 200	0.05 M Citric acid pH 3.5 34 % Polyethylene glycol 200	0.05 M Citric acid pH 3.5 38 % Polyethylene glycol 200	0.05 M Citric acid pH 3.5 42 % Polyethylene glycol 200	0.05 M Citric acid pH 3.5 46 % Polyethylene glycol 200
0.10 M Citric acid pH 3.5 26 % Polyethylene glycol 200	0.10 M Citric acid pH 3.5 30 % Polyethylene glycol 200	0.10 M Citric acid pH 3.5 34 % Polyethylene glycol 200	0.10 M Citric acid pH 3.5 38 % Polyethylene glycol 200	0.10 M Citric acid pH 3.5 42 % Polyethylene glycol 200	0.10 M Citric acid pH 3.5 46 % Polyethylene glycol 200
0.15 M Citric acid pH 3.5 26 % Polyethylene glycol 200	0.15 M Citric acid pH 3.5 30 % Polyethylene glycol 200	0.15 M Citric acid pH 3.5 34 % Polyethylene glycol 200	0.15 M Citric acid pH 3.5 38 % Polyethylene glycol 200	0.15 M Citric acid pH 3.5 42 % Polyethylene glycol 200	0.15 M Citric acid pH 3.5 46 % Polyethylene glycol 200
0.20 M Citric acid pH 3.5 26 % Polyethylene glycol 200	0.20 M Citric acid pH 3.5 30 % Polyethylene glycol 200	0.20 M Citric acid pH 3.5 34 % Polyethylene glycol 200	0.20 M Citric acid pH 3.5 38 % Polyethylene glycol 200	0.20 M Citric acid pH 3.5 42 % Polyethylene glycol 200	0.20 M Citric acid pH 3.5 46 % Polyethylene glycol 200

## Crystallisation Conditions of Figure 4

A: 29 mg/mL Rec/EX + 4 mM IPM, 0.1 M HEPES pH 9.0, 10 % PEG 8000, 4 % Ethylene Glycol

B: 29 mg/mL Rec/EX + 4 mM IPM, 0.1 M HEPES pH 9.4, 10 % PEG 8000, 4 % Ethylene Glycol

C: 46 mg/mL Rec/LG, 1.5 M Ammonium Sulfate, 0.10 M Tris pH 8.5, 12 % Glycerol

D: 46 mg/mL Rec/LG, 5.5 M Ammonium Nitrate, 0.15 M Tris pH 8.5

## Primers

All primers read 5' to 3'.

Original primers, which start and end 10 base pairs from the *leuB* gene:

Forward: GCTGTCGGATCATAAAAGAAAGGAG

Reverse: CTCTACCTAGAGCTAAGACCGCTTA

Second set of primers, which start and end 20 base pairs from the *leuB* gene:

Forward: AAACCACACAGCTGTCGGATCATAA

Reverse: TTTCGATGATTGTTCGAGGCATCAT